CASE STUDY OF NATURAL FLOW AND ARTIFICIAL LIFT FOR A SOLUTION GAS DRIVE RESERVOIR

A

PROJECT

Presented to the Graduate Faculty

of the African University of Science and Technology

in Partial Fulfilment of the Requirements

for the Degree of

MASTER OF SCIENCE IN PETROLEUM ENGINEERING

By

Bismark Osei Bimpong, BSc.

Abuja, Nigeria

December 2009.

CASE STUDY OF NATURAL FLOW AND ARTIFICIAL LIFT FOR A SOLUTION GAS DRIVE RESERVOIR

BY

Bismark Osei Bimpong

RECOMMENDED: …….....

…….....

…….....
Committee Chair

APPROVED: …….....
Chief Academic Officer

…….....
Date

CASE STUDY OF NATURAL FLOW AND ARTIFICIAL LIFT FOR A

SOLUTION

GAS DRIVE RESERVOIR

BY

Bismark Osei Bimpong

RECOMMENDED:

…….....
Chair, Associate Professor Mauricio Prado

…….....
Professor Godwin A. Chukwu

…….....
Professor David Ogbe

APPROVED:

…….....
Chief Academic Officer

…….....
Date

Abstract

Solution gas drive reservoirs are characterized by rapid and continuous decline of reservoir pressure. This rapid and continuous decline of reservoir pressure causes direct decline of reservoir performance at early stages of the life of the reservoir. The principal source of energy which is gas liberation from the crude oil and the subsequent expansion of the solution gas as the reservoir pressure is reduced are inadequate to produce such reservoirs to their full capacities. Ultimate oil recovery from natural flow of a solution - gas drive reservoir makes it one of the least efficient primary recovery mechanisms. This leaves a substantial amount of remaining oil residing in the reservoir which must be produced.

Artificial lift technologies such as continuous gas lift, gas lift with velocity strings and positive displacement pumping is therefore employed at later phases of the reservoir's life to increase the ultimate recovery which is what this project sort to do. Synthetic data based on material balance for a solution – gas drive reservoir is analyzed to predict its primary oil recovery based on which gas lifting, velocity strings technology and positive displacement pumping are suggested to be employed with respect to time at different stages of reservoir's life.

Dedication

To God, to whom I owe all my entirety and accomplishments.

To the sweetest mother on earth, Miss Matilda Quansah, whose prayers and support were significant to its completion. Also, to my one and only sister, Cordelia who sacrificed much for my sake.

God bless us all

Acknowledgements

To the immortal, indefatigable and indomitable God and Savior Jesus Christ be all the praise and adorations. He has been exceedingly gracious and merciful in all that He has done. I say thank you, Abba Father.

Next, I would like to extend my most sincere appreciation to my supervisor, Dr. Mauricio Prado for a wonderful job. He has been extremely patient and kind with all of my shortcomings. His prompt response to problems and criticisms has been the most important reason for the completion of this work.

I have also been helped tremendously by Professor Godwin Chukwu in making sure that my project was always on – going anything he is around. His willingness to proof read this report to make sure that it conforms to acceptable standard is something I appreciate so much. I doff my cap to salute you professor. You are more than a father.

I am also indebted to my fellow second year petroleum engineering students as well as the entire student body for their constant encouragement, moral and financial support in one way or the other. I thank my family for their encouragement and prayer without which this wouldn't have been a reality.

Finally, to my "teaching assistant" who wants her name to be withheld, I say God replenish whatever you may have lost.

Table of Contents

List of Figures

List of Tables

List of Appendices

Appendix **Page**

Nomenclature

P_i	Initial Reservoir Pressure
P	Reservoir pressure
Δp	Change in reservoir pressure = $p_i - p$
P_b	Bubble point pressure
N	Initial (original) oil in place
N_p	Cumulative oil produced
G_p	Cumulative gas produced
W_p	Cumulative water produced
R_p	Cumulative gas – oil ratio
GOR	Instantaneous gas – oil ratio
R_{si}	Initial gas solubility
R_s	Gas Solubility
B_{oi}	Initial oil formation volume factor
B_o	Oil formation volume factor
B_{gi}	Initial gas formation volume factor
B_g	Gas formation volume factor
B_w	Water formation volume factor
ϕ_o, ϕ_g, ϕ_w	PVT related properties which are functions of pressure
Den	Denominator
W_e	Cumulative water influx
W_i	Initial volume of water in the aquifer
m	Ratio of initial gas – cap – gas reservoir volume to initial reservoir oil volume

c_w	Water compressibility
c_f	Formation (rock) compressibility
c_o	Oil compressibility
S_{wc}	Connate water saturation
S_o	Oil saturation
S_o^*	Oil saturation at the beginning of pressure step
S_{oi}	Initial oil saturation
ΔS_o	Change in oil saturation
S_{wi}	Initial water saturation
S_w	Water saturation
$(S_L)_2$	Liquid saturation at the second pressure step
S_g	Gas saturation
P^*	Average reservoir pressure at the beginning of pressure step
P_1	Average reservoir pressure at the first pressure step
P_2	Average reservoir pressure at the second pressure step
G_{p1}	Cumulative gas produced at first pressure step
G_{p2}	Cumulative gas produced at second pressure step
N_{p1}	Cumulative oil produced at first pressure step
N_{p2}	Cumulative oil produced at second pressure step
R_{p2}	Cumulative gas – oil ratio at second pressure step
R_1	Instantaneous gas – oil ratio computed at pressure p_1
R_2	Instantaneous gas – oil ratio computed at pressure p_2
ΔG_p	Change in cumulative gas produced
ΔN_p	Change in cumulative oil produced

N_r	Oil remaining in the reservoir
G_r	Gas remaining in the reservoir
$(GOR)_{avg}$	Average instantaneous gas – oil ratio
GLR_i	Initial gas – liquid ratio
V	Pore volume
X(p), Y(p), Z(p)	Pressure dependent terms
k_{rg}	Gas relative permeability
k_{ro}	Oil relative permeability
μ_o	Oil viscosity
μ_g	Gas viscosity
P_{avg}	Average reservoir pressure
$Q_{o(avg)}$	Average oil flowrate
Q_e	Equivalent oil flowrate
q_e	Equivalent oil flowrate
q_{max}	Maximum oil flowrate
P_{wf}	Bottomhole flowing pressure
q_b	Bubble point flowrate
q	Flowrate
Q_o	Oil flowrate
J*	Starting productivity index
Δt	Change in time
t	Time
F	Underground withdrawal
E_o	Expansion of oil

E_g	Expansion of the gas – cap gas

Chapter 1

1.0 Introduction

1.1 Problem Statement

Solution gas drive also known as Dissolved gas drive or Internal gas drive reservoirs are characterised by a rapid and continuous decline of reservoir pressure. This reservoir pressure behaviour is attributed to the fact that no extraneous fluids or gas caps are available to provide a replacement of the gas and oil withdrawals (Tarek, 2001). This rapid and continuous decline of reservoir pressure causes a direct decline of reservoir performance at early stages of the life of the reservoir. Moreover, the principal source of energy which is gas liberation from the crude oil and the subsequent expansion of the solution gas as the reservoir pressure is reduced are inadequate to produce such reservoirs to their full capacities (Tarek, 2001). Ultimate oil recovery from natural flow of a solution gas drive reservoir (less than 5% to about 30%) makes it one of the least efficient primary recovery mechanisms (Tarek, 2001). The low recovery from this type of reservoir suggests that large quantities of oil remain in the reservoir and, therefore, solution gas drive reservoirs are considered the best candidates for secondary recovery applications.

Artificial lift technologies such as continuous gas lift, gas lift with velocity strings and positive displacement pumping method is therefore employed at later phases of the reservoir in order to increase the ultimate recovery. The main challenge is to know when to change existing production mechanism to a new one for optimum recovery. A production design has therefore been made in an attempt to solving this problem with respect to constraints such as maximum production rate, maximum drawdown, and available gas lift.

The flowing bottom-hole pressure required to lift the fluids up to the surface may be influenced by size of the tubing string (Lyons, 1996) and for that matter the time when tubing strings should be replaced as a function of cumulative production is necessary.

1.2 Method of Conducting the Project

Designing the natural flow and artificial lift tubing strings for the whole life of a well forms the tasks of this project. This is based on certain constraints such as maximum production rate, maximum drawdown, and available gas lift and horsepower requirement. Synthetic reservoir performance based on a material balance is the main data source for this project. A forecast of the production of oil as well as the time when tubing strings should be replaced as a function of the cumulative production is proposed.

1.3 Objectives

The objectives of this project are to:

- Design natural flow and artificial lift tubing strings for the whole life of a well.
- Forecast the production of oil as well as the time when tubing strings should be replaced as a function of both cumulative production and time.

1.4 Outline of this Project

The project consists of five (5) chapters. Chapter 1 defines the problem at hand, the method which the project follows and objectives. Chapter 2 presents a literature review of the topic as well as the technical terms that make up the topic. Chapter 3 introduces a thorough review of the material balance equation, methods of predicting primary oil recovery with emphasis on Muskat's method which has been employed in this report. Application of the Muskat's method is illustrated with a synthetic reservoir data. Chapter 4 comes up with the natural flow design as well as the artificial lift tubing strings with respect to the set constraints. Gas lift with velocity strings and suggestion for a positive displacement pumping method for later phases of the reservoir are also presented. In summary, a forecast of the production and time when tubing strings should be replaced as a function of cumulative production is suggested. Chapter 5 gives a summary and conclusions stemming from this project and provides recommendations for future research work in this area. This work focuses on applying artificial lift technology, in this case gas lift, to help a well to meet its recommended flow capacity.

Chapter 2

2.0 Literature Review

The Inflow Performance Relationship (IPR) describes the behaviour of a well's flowing pressure and production rate, which is an important tool in understanding the reservoir or well behaviour and quantifying the production rate. The IPR is often required for designing well completion, optimizing well production, nodal analysis calculations, and designing artificial lift. Different IPR correlations exist today in the petroleum industry with the most commonly used models being that of Vogel's and Fetkovich's (Mohammed et al, 2009).

2.1 Reservoir Natural Drive Mechanisms

Natural drive mechanisms refer to the energy in the reservoir that allows the fluid to flow through the porous network and into the wells. In its simplest definition, reservoir energy is always related to some kind of expansion (Cosentino, 2001). For a proper understanding of reservoir behaviour and predicting future performance, it is necessary to have knowledge of the driving mechanisms that control the behaviour of fluids within reservoirs. Several types of expansions take place inside and outside the reservoir, as a consequence of fluid withdrawals. Inside the reservoir, the expansion of hydrocarbons, connate water and the rock itself provides energy for the fluid to flow. Outside the producing zone, the expansion of a gas cap and/or of an aquifer may also supply significant amount of energy to the reservoir. In this case, the expansion of an external phase causes its influx into the reservoir and will ultimately result in a displacement process (Cosentino, 2001). There are basically six driving mechanisms that provide the natural energy necessary for oil recovery:

- Rock and liquid expansion drive
- Depletion drive

- Gas cap drive
- Water drive
- Gravity drainage drive
- Combination drive

The figures 2.1 and 2.2 below compare various characteristics of the drive mechanisms.

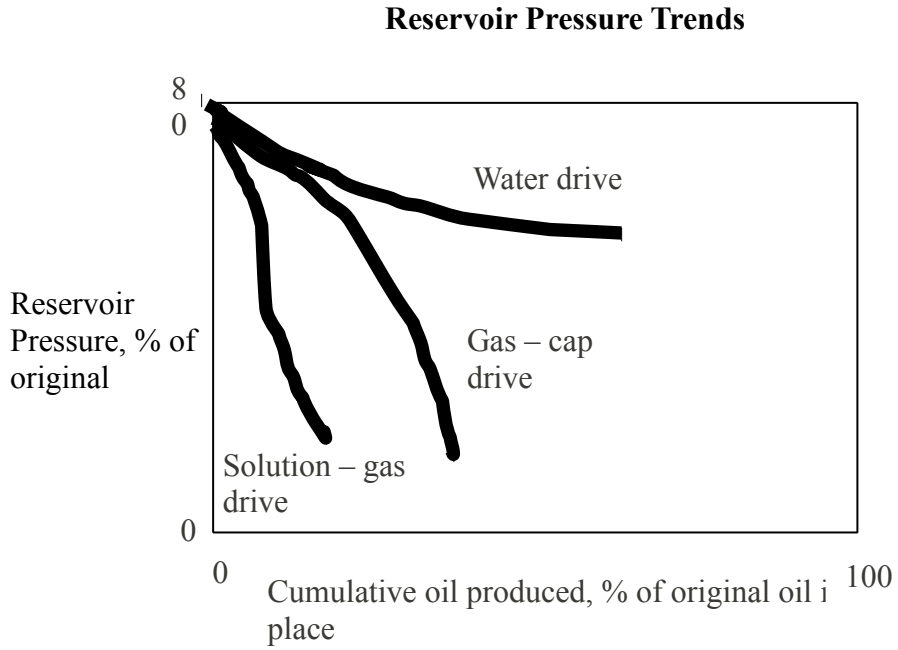

Figure 2.1: Typical pressure trends of some drive mechanisms

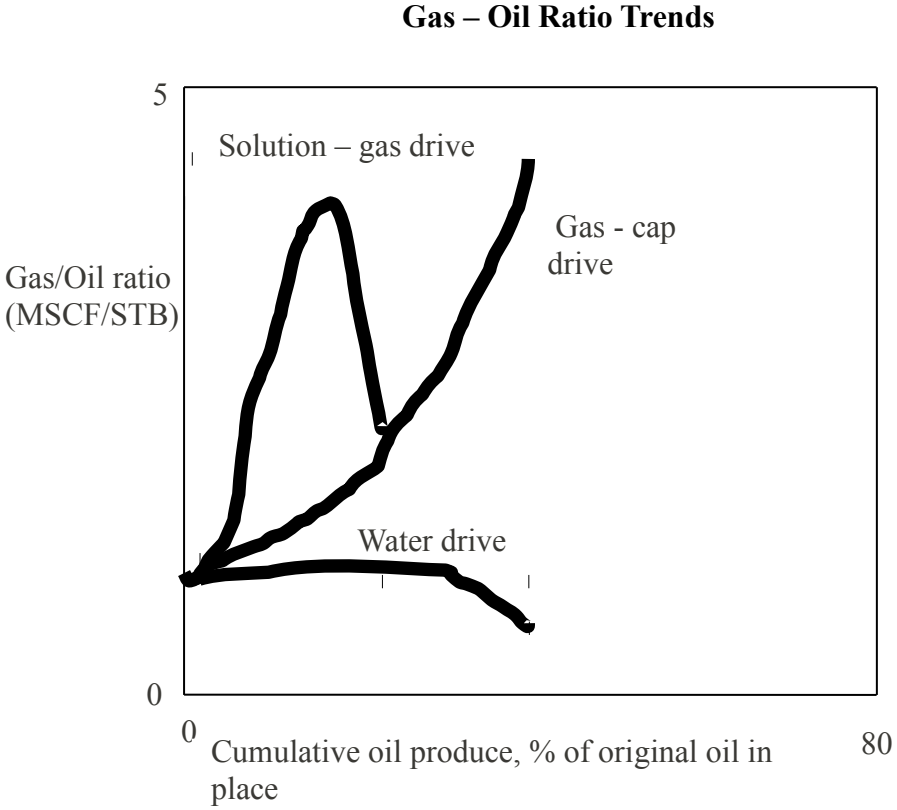

Figure 2.2: Typical Gas – Oil Ratio Trends of Some Drive Mechanisms

The attention of this project is on the Depletion drive mechanism also known as the solution gas drive mechanism which is reviewed as follows.

2.2 Solution – Gas Drive Reservoir

This driving form may also be referred to by the following various terms: Solution gas drive, Dissolved gas drive or Internal gas drive. A solution gas drive reservoir is one in which the principal drive mechanism is the expansion of the oil and its originally dissolved gas. The increase in fluid volumes during the process is equivalent to the production (Dake, 1978). A solution – gas drive reservoir is mostly closed from any outside source of energy, such as water encroachment. Its pressure is initially above bubble-point pressure, and, therefore, no free gas exists. The only source of material to replace the produced fluids is the expansion of the fluids remaining in the reservoir

(Beggs, 2003). Some small but usually negligible expansion of the connate water and rock may also occur.

When the reservoir falls below the saturation pressure, gas is liberated from the hydrocarbon liquid phase. Expansion of the gas phase contributes to the displacement of the residual liquid phase. Initially the liberated gas will expand but not flow, until its saturation reaches a threshold value, called critical gas saturation (Cosentino, 2001). Typical values of the critical saturation ranges between 2 and 10% (Cosentino, 2001). When this value is reached, gas starts to flow with a velocity proportional to its saturation. The more the pressure drops, the faster the gas is liberated and produced, thus lowering further the pressure, in a sort of chain reaction that quickly leads to the depletion of the reservoir (Cosentino, 2001).

At the surface, solution gas drive reservoirs are characterised in general by rapidly increasing in Gas – Oil Ratios (GORs) and decreasing oil rates. Generally no or little water is produced. The ideal behaviour of a field under solution gas drive is depletion is illustrated in figure 2.3. The GOR curve has a peculiar shape, in that it tends to remain constant and equal to the initial R_{si} while the reservoir pressure is below the bubble point, then it tends to decline slightly until the critical gas saturation is reached. This decline corresponds to the existence of some gas in the reservoir that cannot be mobilized (Cosentino, 2001). After the critical saturation is reached, the GOR increases rapidly and finally declines towards the end of the field life, when the reservoir approaches the depletion pressure.

The most important parameter in solution – gas drive reservoirs is gas – oil relative permeability (Cosentino, 2001). Actually, the increase in the GOR curve is related to the increased gas permeability with respect to oil, as its saturation increases. The lower the critical gas saturation, the more rapidly the gas will be mobilised and produced, thus accelerating the depletion and impairing the final recovery (Cosentino, 2001).

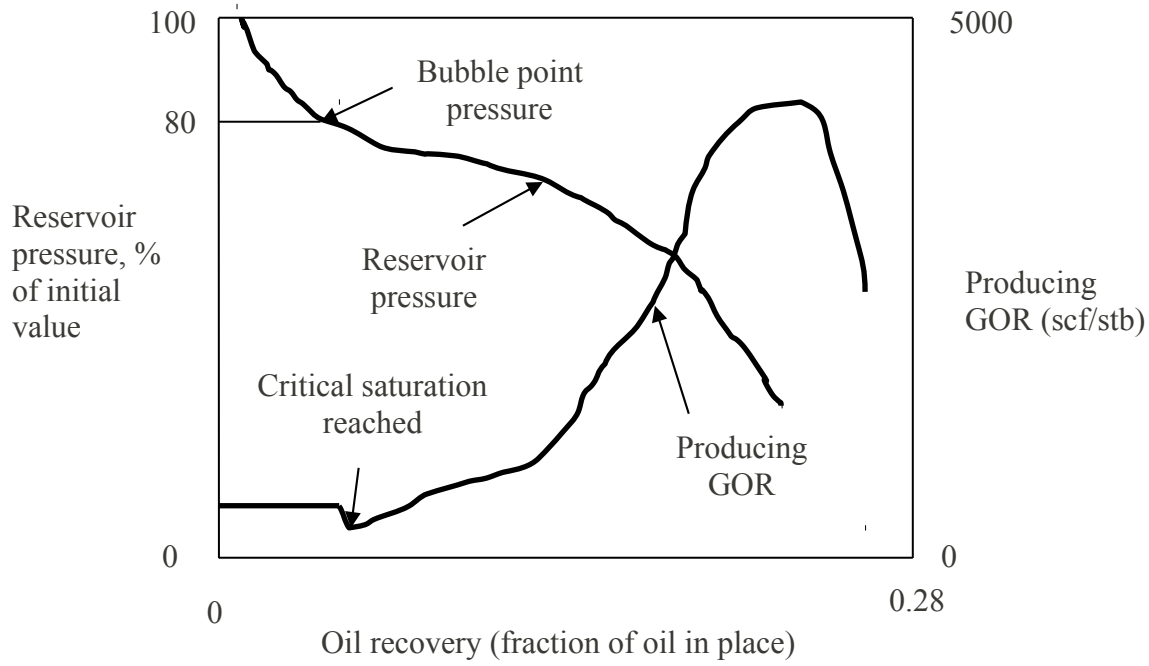

Figure 2.3: Ideal production behaviour of a solution gas drive reservoir

2.3 Material Balance for some Drive Mechanisms

Material balance has long been regarded as one of the basic tools of reservoir engineers for interpreting and predicting reservoir performance (Dake, 2001). In the most elementary form the material balance equation states that the initial volume in place equals the sum of the volume remaining and the volume produced (Lyons, 1996). The zero dimensional material balance is derived and subsequently applied in this report, using mainly the interpretative technique of Havlena and Odeh, to gain an understanding of reservoir drive mechanisms under primary recovery conditions (Dake, 2001).

$$N_p\left(B_o+\left(R_p-R_s\right)B_g\right)=NB_{oi}\left[\frac{\left(B_o-B_{oi}\right)+\left(R_{si}-R_s\right)B_g}{B_{oi}}+m\left(\frac{B_g}{B_{gi}}-1\right)+\left(1+m\right)\left(\frac{c_w S_{wc}+c_f}{1-S_{wc}}\right)\Delta p\right]$$
$$+\left(W_e-W_p\right)B_w$$

(2.1)

According to Tarek, 2001, the basic assumptions in the material balance equation are as follows:

- **Constant temperature:** Pressure - volume changes in the reservoir are assumed to occur without any temperature changes.
- **Pressure equilibrium:** All parts of the reservoir have the same pressure, and fluid properties are therefore constant throughout.
- **Constant production data:** All production data should be recorded with respect to the same time period.
- **Constant reservoir volume:** Reservoir volume is assumed to be constant except for those conditions of rock and water expansion of water influx that are specifically considered in the equation.

2.3.1 Solution – Gas Drive

A schematic representation of material balance equations for solution gas reservoirs, when the change in pore volume is negligible is shown in figure 2.4 (Lyons, 1996). Above the bubble point, the drive energy is due to the expansion of the undersaturated, single phase oil, the connate water expansion and the pore compaction, while below, the complex solution gas drive process is activated once gas has been liberated from the oil (Dake, 2001).

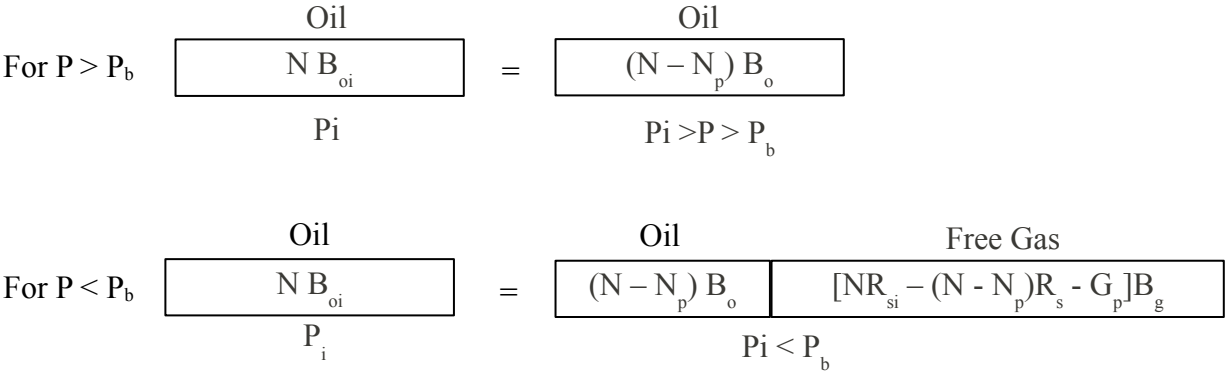

Figure 2.4: Schematic of material balance equations for solution – gas drive reservoir (**Source:** Lyon, 1996)

Two main phases of a solution gas drive reservoir are identified. These are depletion above the bubble point and depletion below the bubble point.

Depletion above bubble point (Undersaturated)

For a solution gas drive reservoir it is assumed that there is no initial gas cap, thus m = 0, and that the aquifer is relatively small in volume and the water influx is negligible. Furthermore, above the bubble point, $R_s = R_{si} = R_p$, since all the gas produced at the surface must have been dissolved in the oil in the reservoir (Dake, 2001). Under these assumptions, the material balance equation (2.1) becomes:

$$N_p B_o = N B_{oi}\left(\frac{(B_o - B_{oi})}{B_{oi}} + \frac{(c_w S_{wc} + c_f)}{1 - S_{wc}}\Delta p\right) \qquad (2.2)$$

The component describing the reduction in the hydrocarbon pore volume, due to the expansion of the connate water and reduction in pore volume cannot be neglected for an undersaturated oil reservoir since the compressibilities c_w and c_f are generally of the same order of magnitude as the compressibility of the oil (Dake, 2001) where the oil compressibility is given by:

$$c_o = \frac{(B_o - B_{oi})}{B_{oi}\Delta p} \qquad (2.3)$$

Substituting eqn. (2.3) into eqn. (2.2) gives

$$N_p B_o = N B_{oi}\left(c_o \frac{(c_w S_{wc} + c_f)}{1 - S_{wc}}\right)\Delta p \qquad (2.4)$$

Since there are only two fluids in the reservoir, that is , oil and water, then the sum of the fluid saturations must be 100% of the pore volume, or

$$S_o + S_{wc} = 1 \tag{2.5}$$

and substituting eqn. (2.5) into eqn. (2.4) gives the reduced form of the material balance as:

$$N_p B_o = NB_{oi}\left(\frac{\left(c_o S_o + c_w S_{wc} + c_f\right)}{1 - S_{wc}}\right)\Delta p \tag{2.6}$$

or $$N_p B_o = NB_{oi} c_o \Delta p \tag{2.7}$$

where

$$c_o = \frac{1}{1 - S_{wc}}\left(c_o S_o + c_w S_{wc} + c_f\right)$$

is the effective, saturation – weighted compressibility of the reservoir system.

Depletion below bubble point (Saturated oil)

For a solution gas drive reservoir, below the bubble point, the following are assumed:

m = 0; no initial gas cap

negligible water influx

the term $NB_{oi}\left(\frac{\left(c_w S_{wc} + c_f\right)}{1 - S_{wc}}\right)\Delta p$ is negligible once a significant free gas saturation develops in the reservoir.

Under these conditions the material balance equation can be simplified as

$$N_p\left(B_o+\left(R_p-R_s\right)B_g\right)=N\left(\left(B_o-B_{oi}\right)+\left(R_{si}-R_s\right)B_g\right) \qquad (2.8)$$

2.3.2 Gas Cap Drive

For a reservoir in which gas cap drive is the predominant mechanism it is still assumed that the natural water influx is negligible ($W_e = 0$) and, in the presence of so much high compressibility gas, that the effect of water and pore compressibilities is also negligible (Dake, 2001). Under these circumstances, the material balance eqn. (2.1), can be written as

$$N_p\left(B_o+\left(R_p-R_s\right)B_g\right)=NB_{oi}\left[\frac{\left(B_o-B_{oi}\right)+\left(R_{si}-R_s\right)B_g}{B_{oi}}+m\left(\frac{B_g}{B_{gi}}-1\right)\right] \qquad (2.9)$$

Using the technique of Havlena and Odeh with negligible water influx, the material balance equation can be reduced to the form

$$F=N\left(E_o+mE_g\right) \qquad (2.10)$$

2.3.3 Water Drive

A drop in the reservoir pressure, due to the production of fluids, causes the aquifer water to expand and flow into the reservoir. Applying compressibility definition to the aquifer, then

$$\text{Water Influx} = \text{Aquifer Compressibility} \times \text{Initial Volume of Water} \times \text{Pressure Drop}$$

or

$$W_e=\left(c_w+c_f\right)W_i\Delta p \qquad (2.11)$$

Using the technique of Havlena and Odeh (assuming that B_w = 1), the full material balance can be expressed as

$$F = N\left(E_o + mE_g + E_{f,w}\right) + W_e \qquad (2.12)$$

If the reservoir has no initial gas cap and coupled with the fact that water and pore compressibilities are small and also the water influx helps to maintain the reservoir pressure (making Δp appearing in the $E_{f,w}$ term reduced), eqn. (2.12) reduces to

$$F = NE_o + W_e \qquad (2.13)$$

2.4 Predicting Primary Recovery in Solution – Gas Drive Reservoirs

Several methods for predicting performance of solution-gas behaviour relating pressure decline to gas-oil ratio and oil recovery have appeared in literature (Lyons, 1996). These methods include Tracy's method, Tarner's method and Muskat's method. The following assumptions are generally made: uniformity of the reservoir at all times regarding porosity, fluid saturations, and relative permeabilities; uniform pressure throughout the reservoir in both the gas and oil zones (which means the gas and oil volume factors, the gas and oil viscosities, and the solution gas will be the same throughout the reservoir); negligible gravity segregation forces; equilibrium at all times between the gas and the oil phases; a gas liberation mechanism which is the same as that used to determine the fluid properties, and no water encroachment and negligible water

production (Lyons, 1996).

2.4.1 Tracy's Method

Neglecting the formation and water compressibilities as well as any form of injection, the general material balance equation as expressed by eqn. 2.1 can be reduced to (Tarek, 2001)

$$N=\frac{N_p B_o+\left(G_p-N_p R_s\right)B_g-\left(W_e-W_p B_w\right)}{\left(B_o-B_{oi}\right)+\left(R_{si}-R_s\right)B_g+mB_{oi}\left[\frac{B_g}{B_{gi}}-1\right]} \qquad (2.14)$$

where $G_p=R_p N_p$

Tracy (1955) suggested that the above relationship can be rearranged into a more usable form as:

$$N=N_p \Phi_o+G_p \Phi_g+\left(W_p B_w-W_e\right)\Phi_w \qquad (2.15)$$

where ϕ_o, ϕ_g and ϕ_w are considered PVT related properties that are functions of pressure and defined by:

$$\Phi_o=\frac{B_o-R_s B_g}{Den} \qquad (2.16)$$

$$\Phi_g=\frac{B_g}{Den} \qquad (2.17)$$

$$\Phi_w=\frac{1}{Den} \qquad (2.18)$$

with

$$Den=\left(B_o-B_{oi}\right)+\left(R_{si}-R_s\right)B_g+mB_{oi}\left[\frac{B_g}{B_{gi}}-1\right] \qquad (2.19)$$

Figure 2.5 gives a graphical presentation of the behaviour of Tracy's PVT functions with changing pressure (Tarek, 2001).

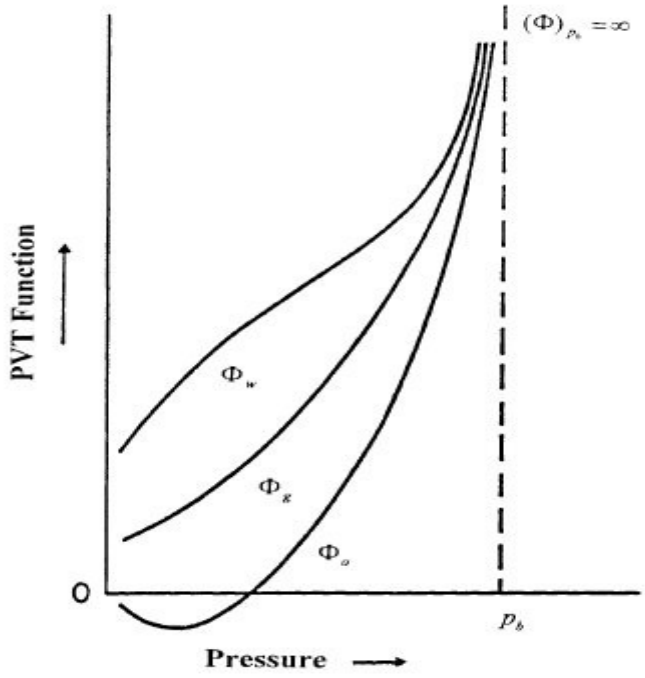

Figure 2.5: Tracy's PVT functions

(**Source:** Tarek, 2001)

For a solution gas drive reservoir, equations (2.15) and (2.19) reduce to the following equations respectively:

$$N=N_p \Phi_o+G_p \Phi_g \tag{2.20}$$

and

$$Den=\left(B_o-B_{oi}\right)+\left(R_{si}-R_s\right)B_g \tag{2.21}$$

Tracy's calculations are performed in series of pressure drops that proceed from known reservoir condition at the previous reservoir pressure p^* to the new assumed lower pressure p. The calculated results at the new reservoir pressure become "known" at the next assumed lower pressure (Tarek, 2001).

2.4.2 Tarner's Method

This is a trial and error procedure based on the simultaneous solution of the material balance equation and the instantaneous gas-oil ratio equation (Lyons, 1996). For a pressure drop from p_1 to p_2, the procedure involves a stepwise calculation of cumulative oil produced $(Np)_2$ and of cumulative gas produced $(Gp)_2$. The stepwise procedure as enumerated in Lyons, 1996 is as follows:

- During the pressure drop from p_1 to p_2, assume that the cumulative oil production increases from $(Np)_1$ to $(Np)_2$. At the bubble point pressure, Np should be set equal to zero.
- By means of the material-balance equation for $W_p = 0$, compute the cumulative gas produced $(GP)_2$ at pressure p_2 as:

$$\left(G_p\right)_2=\left(N_p\right)_2\left(R_p\right)_2=N\left[\left(R_{si}-R_s\right)-\frac{B_{oi}-B_o}{B_g}\right]-\left(N_p\right)_2\left(\frac{B_o}{B_g}-R_s\right) \tag{2.22}$$

- Compute the fractional total liquid saturation $(S_L)_2$ at pressure p_2 as:

$$(S_L)_2 = S_w + (1 - S_w)\frac{B_o}{B_{oi}}\left[1 - \frac{(N_p)_2}{N}\right] \qquad (2.23)$$

- Determine the k_{rg}/k_{ro} ratio corresponding to the total liquid saturation $(S_L)_2$ and compute the instantaneous gas – oil ratio at p_2 as:

$$R_2 = R_s + \left(\frac{k_{rg}}{k_{ro}}\right)\left(\frac{\mu_o B_o}{\mu_g B_g}\right) \qquad (2.24)$$

- Compute the cumulative gas produced at pressure p_2 as:

$$\left(G_p\right)_2 = \left(G_p\right)_1 + \frac{R_1 + R_2}{2}\left[\left(N_p\right)_2 - \left(N_p\right)_1\right] \qquad (2.25)$$

where R_1 is the instantaneous gas – oil ratio computed at pressure p_1.

2.4.3 Muskat's Method

Muskat expresses the material balance in terms of finite pressure differences in small increments. The changes in variables that affect production are evaluated at any stage of depletion or pressure (Lyons, 1996). Assumption is made that values of the variables will hold for a small drop in pressure, and the incremental recovery can be calculated for the small pressure drop (Lyons, 1996). Knowing PVT data and the gas- oil relative permeabilities at any liquid saturation, the unit recovery by pressure depletion can be computed from a differential form of the material balance equation as:

$$\frac{dS_o}{dp}=\frac{\frac{S_o B_g}{B_o}\frac{dR_s}{dp}+\frac{S_o}{B_o}\frac{k_{rg}\mu_o}{k_{ro}\mu_g}\frac{dB_o}{dp}+\left(1-S_o-S_w\right)B_g\frac{d\left(1/\mathrm{B}_g\right)}{dp}}{1+\frac{k_{rg}\mu_o}{k_{ro}\mu_g}} \quad (2.26)$$

From the change in saturation at any pressure, the reservoir saturation at that time can be related to the change in oil production and the instantaneous gas – oil ratio (Lyons, 1996). Using ($\Delta S_o/\Delta p$) which is mostly the average, the oil saturation S_o is computed as:

$$S_o=S_o*-(p*-p)\left(\frac{\Delta S_o}{\Delta p}\right)_{avg} \quad (2.27)$$

The cumulative oil production is then calculated as:

$$N_p=N\left[1-\left(\frac{B_{oi}}{B_o}\right)\left(\frac{S_o}{1-S_{wi}}\right)\right] \quad (2.28)$$

And the cumulative gas production is computed as:

$$G_p=G_p+\Delta G_p \quad (2.29)$$

where $\Delta G_p=(GOR)_{avg}\Delta N_p$ (2.30)

Application of the Muskat's method in predicting primary recovery in solution gas drive reservoir is further developed in chapter 3.

2.5 Artificial Lift Methods

Most oil reservoirs are of the volumetric type where the driving mechanism is the expansion of solution gas when reservoir pressure declines because of fluid production. Oil reservoirs will eventually not be able to produce fluids at economical rates unless natural driving mechanisms (e.g., aquifer and/or gas cap) or pressure maintenance mechanisms (e.g., water flooding or gas injection) are present to maintain reservoir energy (Boyun et al., 2007). When reservoir pressure is insufficient to sustain the flow of oil to the surface at adequate rates, natural flow must be aided by artificial lift. There are two basic forms of artificial lift: continuous gas lift and bottomhole pumping (Golan and Whitson, 1995). Both methods supplement the natural drive energy of the reservoir and increase the flow by reducing backpressure at the wellbore caused by flowing fluids in the tubing (Golan and Whitson, 1995). Approximately 50% of wells worldwide need artificial lift systems (Boyun et al., 2007).

The commonly used artificial lift methods include the following:

- Sucker rod pumping
- Continuous Gas lift
- Intermittent Gas Lift
- Electrical submersible pumping
- Hydraulic piston pumping
- Hydraulic jet pumping
- Plunger lift
- Progressing cavity pumping

In naturally flowing wells, the well flowrate capacity is usually higher than the recommended or desired flowrate and the well production is controlled by the use of a choke. There are some naturally flowing wells that although able to produce steadily the desired flowrate, can not start production without some help. Those wells need a kick-off operation after a shut down in order to produce a steady flowrate. In this case an artificial lift method can be used whenever necessary to kick-off the well (Prado, 2008).

In certain cases, the bottom hole flowing pressure may be sufficient only to produce the well at flowrates smaller than the recommended or desired flowrate. In some cases the bottom hole flowing pressure may not be capable to produce any flowrate at all and the well is called a dead well. In those two cases artificial lift methods can be used to achieve the recommended flowrate (Prado, 2008).

Finally, there are conditions when the bottom hole flowing pressure is able to produce the fluids to the surface but the production is unsteady. In those cases artificial lift methods can be used to stabilize the well (Prado, 2008).

Artificial lift is the area of petroleum engineering related to the use of technologies to promote an increase in the production rate of flowing oil or gas wells, to put wells back into production or to stabilize production by using an external horsepower source. The external source helps the bottom hole flowing pressure to overcome the pressure drops in the system downstream of the perforations or to use methods that reduce the pressure drop in the production system by improving the multiphase flow conditions in the well. In any case either energy or products will be consumed at the surface (costs) to obtain higher flowrates from the well (income). The main purpose of artificial lift is to increase the profit of the operation (Prado, 2008).

2.5.1 Gas Lift

Gas lift technology increases oil production rate by injection of compressed gas into the lower section of tubing through the casing–tubing annulus and an orifice installed in the tubing string (Boyun et al., 2007). Upon entering the tubing, the compressed gas affects liquid flow in two ways: (a) the energy of expansion propels (pushes) the oil to the

surface and (b) the gas aerates the oil so that the effective density of the fluid is less and, thus, easier to get to the surface (Boyun et al., 2007). Gas lift technology is a simple and flexible method seen as an extension of natural flow. It mostly requires a source of high pressure gas and casing and lines must withstand injection pressure (Prado, 2008).

A continuous gas lift operation is a steady-state flow of the aerated fluid from the bottom (or near bottom) of the well to the surface. In continuous gas lift, a small volume of high-pressure gas is introduced into the tubing to aerate or lighten the fluid column. This allows the flowing bottom-hole pressure with the aid of the expanding injection gas to deliver liquid to the surface. To accomplish this efficiently, it is desirable to design a system that will permit injection through a single valve at the greatest depth possible with the available injection pressure (Boyun et al., 2007). Intermittent gas lift operation is characterized by a start-and-stop flow from the bottom (or near bottom) of the well to the surface. This is unsteady state flow (Boyun et al., 2007). The type of gas lift operation used, continuous or intermittent, is also governed by the volume of fluids to be produced, the available lift gas as to both volume and pressure, and the well reservoir's conditions such as the case when the high instantaneous BHP drawdown encountered with intermittent flow would cause excessive sand production, or coning, and/or gas into the wellbore (Boyun et al., 2007). A complete gas lift system consists of a gas compression station, a gas injection manifold with injection chokes and time cycle surface controllers, tubing string with installations of unloading valves and operating valve, and a down-hole chamber (Boyun et al., 2007). Figure 2.5 shows the configuration of a typical gas lift well.

Gas Lift with Velocity Strings

Velocity strings are a commonly applied remedy to liquid loading in gas wells (Oudeman, 2007). By installing a small diameter string inside the tubing, the flow area is reduced which increases the velocity and restores liquid transport to surface. The disadvantage of the velocity string is the increase in frictional pressure drop, constraining production. Hence an optimal velocity string has to be selected such that liquid loading is delayed

over a long period with a minimal impact on production (Oudeman, 2007). This requires accurate methods to predict pressure drop in the velocity string as well as tubing-velocity string annulus (Oudeman, 2007).

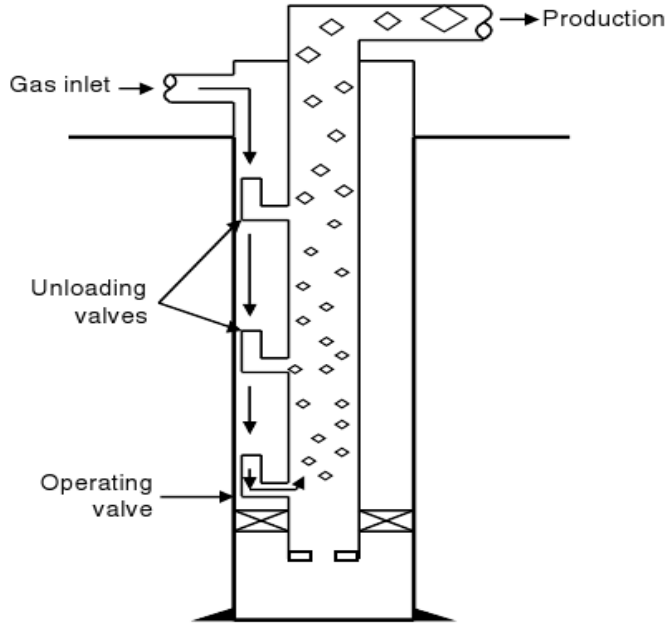

Figure 2.6: Configuration of a typical gas lift well
(**Source:** Boyun et al., 2007)

2.5.2 Bottomhole Pumping

Bottomhole pumping provides mechanical energy to lift oil from bottom hole to surface. It raises the pressure in a liquid by transforming mechanical work into potential energy, that is, pressure. Liquid enters the pump at a given pressure, called discharge pressure. Pump pressure usually refers to the difference between the discharge and the suction pressures (Golan and Whitson, 1995). Pump pressure corresponds to the gain in potential energy of the liquid. This gain represents only a fraction of the total work used to drive a pump. It is efficient, simple, and easy for field people to operate. It can pump a well down to very low pressure to maximize oil production rate (Boyun et al., 2007). The efficiency of a pump depends on how efficiently it can transform the driving forces into

fluid potential energy (Golan and Whitson, 1995).

Pumps are generally classified according to the physical principle used to transform driving forces into pressure (Golan and Whitson, 1995). The main classes of conventional pumps are: positive – displacement and dynamic – displacement pumps. Positive – displacement pumps develop pressure by moving a piston or cam to reduce the volume of a compression chamber. This compression raises the pressure of liquid in the chamber (Golan and Whitson, 1995). Dynamic – displacement pumps develop pressure by a sequence of accelerations and decelerations of the pumped liquid (Golan and Whitson, 1995).

Positive – Displacement Pumps

1. *Sucker Rod Pump:* a positive – displacement pump that compresses liquid by the reciprocating motion of a piston. The piston is actuated by a string of sucker rods that extend from the bottomhole pump to the pumping unit at the surface (Golan and Whitson, 1995).

2. *Reciprocating Hydraulic Pump:* a positive – displacement pump with a reciprocating piston. The piston is actuated by a reciprocating hydraulic motor coupled and assembled with the pump. The downhole motor is driven by a power fluid injected at high pressure from the surface (Golan and Whitson, 1995).

Centrifugal submersible pump and jet pump are examples of dynamic – displacement pumps.

Chapter 3

3.0 Material Balance for Predicting Primary Recovery

3.1 Muskat Material Balance in Predicting Primary Recovery

From Dake, 1994, consider an initially saturated gas reservoir from which *Np* (stb) of oil have been produced. Then the oil remaining in the reservoir at that stage of depletion is:

$$N_r = N - N_p = \frac{VS_o}{B_o} \quad (\text{stb}) \tag{3.1}$$

where *V* is the pore volume (rb). The change in this volume with pressure is:

$$\frac{dN_r}{dp} = V\frac{1}{B_o}\frac{dS_o}{dp} - V\frac{S_o}{B_{o^2}}\frac{dB_o}{dp} \tag{3.2}$$

The total volume of dissolved and free gas in the reservoir is:

$$G_r = V\frac{S_o R_s}{B_o} + \left(1 - S_o - S_{wc}\right)\frac{V}{B_g} \quad (\text{stb}) \tag{3.3}$$

And its change in volume with pressure is:

$$\frac{dG_r}{dp} = V\left(\frac{S_o}{B_o}\frac{dR_s}{dp} + \frac{R_s}{B_o}\frac{dS_o}{dp} - \frac{R_s S_o}{B_{o^2}}\frac{dB_o}{dp} - \frac{1}{B_g}\frac{dS_o}{dp} - \frac{1 - S_o - S_{wc}}{B_{g^2}}\frac{dB_g}{dp}\right) \tag{3.4}$$

The instantaneous GOR while producing at this stage of depletion can be obtained by dividing equation (3.4) by (3.2) to give:

$$R=\frac{\frac{S_o}{B_o}\frac{dR_s}{dp}+\frac{R_s}{B_o}\frac{dS_o}{dp}-\frac{R_sS_o}{B_{o^2}}\frac{dB_o}{dp}-\frac{1}{B_g}\frac{dS_o}{dp}-\frac{1-S_o-S_{wc}}{B_{g^2}}\frac{dB_g}{dp}}{\frac{1}{B_o}\frac{dS_o}{dp}-\frac{S_o}{B_{o^2}}\frac{dB_o}{dp}} \qquad (3.5)$$

An alternative expression for the producing GOR can be obtained by applying Darcy's law for gas/oil flow in the reservoir as:

$$GOR=R_s+\frac{k_{rg}}{B_g}\frac{B_o}{k_{ro}}\frac{\mu_o}{\mu_g} \quad (\text{scf/stb}) \qquad (3.6)$$

in which k_{rg} and k_{ro} are the relative permeabilities to oil and gas. Equation (3.5) and (3.6) can be equated and solved to give the oil saturation derivative with respect to pressure as:

$$\frac{dS_o}{dp}=\frac{\frac{S_oB_g}{B_o}\frac{dR_s}{dp}+\frac{S_o}{B_o}\frac{k_{rg}}{k_{ro}}\frac{\mu_o}{\mu_g}\frac{dB_o}{dp}+\left(1-S_o-S_{wc}\right)B_g\frac{d\left(1/B_g\right)}{dp}}{1+\frac{k_{rg}}{k_{ro}}\frac{\mu_o}{\mu_g}} \qquad (3.7)$$

with

$$\Delta S_o=S_o*-S_o$$

$$\Delta p=p*-p$$

where S_o^*, p^* = oil saturation and average reservoir pressure at the beginning of the pressure step

S_o, p = oil saturation and average reservoir pressure at the end of the time step

R_s = gas solubility, scf/stb

B_g = gas formation volume factor, bbl/scf

Craft et al, 1991, suggested the calculations can be greatly facilitated by computing and preparing in advance in graphical form the following pressure dependent groups:

$$X(p)=\frac{B_g}{B_o}\frac{dR_s}{dp} \tag{3.8}$$

$$Y(p)=\frac{1}{B_o}\frac{\mu_o}{\mu_g}\frac{dB_o}{dp} \tag{3.9}$$

$$Z(p)=B_g\frac{d(1/B_g)}{dp} \tag{3.10}$$

Introducing the above pressure dependent terms into equation (3.7) gives:

$$\frac{\Delta S_o}{\Delta p}=\frac{S_o X(p)+S_o\frac{k_{rg}}{k_{ro}}Y(p)+(1-S_o-S_{wc})Z(p)}{1+\frac{k_{rg}}{k_{ro}}\frac{\mu_o}{\mu_g}} \tag{3.11}$$

Craft et al, 1991 proposed the following procedure for solving Muskat's equation fro a given pressure drop Δp, that is, (p^* - p).

The procedure is as follows:

Step 1: Prepare a plot of k_{rg}/k_{ro} versus gas saturation.

Step 2: Plot R_s, B_o and $(1/B_g)$ versus pressure and determine the slope of each plot at selected pressures, that is, dB_o/dp. dR_s/dp and $d(1/B_g)/dp$.

Step 3: Calculate the pressure dependent terms $X(p)$, $Y(p)$ and $Z(p)$ that correspond to the selected pressures in step 2.

Step 4: Plot the pressure dependent terms as a function of pressure.

Step 5: Graphically determine the values of *X(p)*, *Y(p)* and *Z(p)* that corresponds to the pressure *p*.

Step 6: Solve equation (3.11) for $(\Delta S_o/\Delta p)$ by using the oil saturation S_o^* at the beginning of the pressure drop interval p^*.

Step 7: Determine the oil saturation S_o at the average reservoir pressure *p*, from:

$$S_o = S_o - (p - p)\left(\frac{\Delta S_o}{\Delta p}\right) \tag{3.12}$$

Step 8: Using the S_o from step 7 and the pressure p, recalculate $(\Delta S_o/\Delta p)$ from equation (3.11).

Step 9: Calculate the average value for $(\Delta S_o/\Delta p)$ from the two values obtained in step 6 and 8, or:

$$\left(\frac{\Delta S_o}{\Delta p}\right)_{\text{avg}} = \frac{1}{2}\left[\left(\frac{\Delta S_o}{\Delta p}\right)_{\text{step 6}} + \left(\frac{\Delta S_o}{\Delta p}\right)_{\text{step 8}}\right] \tag{3.13}$$

Step 10: Using $(\Delta S_o/\Delta p)_{avg}$, solve for the oil saturation S_o from:

$$S_o = S_o - (p - p)\left(\frac{\Delta S_o}{\Delta p}\right)_{\text{avg}} \tag{3.14}$$

This value of S_o becomes S_o^* for the next pressure drop interval.

Step 11: Calculate gas saturation S_g by:

$$S_g = 1 - S_{wi} - S_o \tag{3.15}$$

Step 12: Using the saturation equation, that is, equation (3.17), solve for the cumulative oil production.

$$N_p = N\left[1 - \left(\frac{B_{oi}}{B_o}\right)\left(\frac{S_o}{1 - S_{wi}}\right)\right] \tag{3.16}$$

The saturation equation is given by:

$$S_o = (1 - S_{wi})\left(1 - \frac{N_p}{N}\right)\frac{B_o}{B_{oi}} \tag{3.17}$$

Step 13: Calculate the cumulative gas production *Gp* as:

$$G_p = G_p + (GOR)_{avg}\Delta N_p \tag{3.18}$$

where $(GOR)_{avg}$ is given by:

$$(GOR)_{avg} = \frac{GOR + GOR}{2} \tag{3.19}$$

Step 14: Repeat steps 5 through 13 for all pressure drops of interest.

This procedure is used in predicting the primary oil recovery using synthetic data from a solution gas drive reservoir for this project.

3.2 Application of Muskat's Method in Predicting Oil Recovery

Consider a volumetric depletion drive reservoir that exists at its bubble point pressure of 2500 psi with relevant reservoir data provided. Also, detailed fluid property data are listed for the various pressure depletion steps as follows:

Given

Initial Reservoir Pressure ($p_i = p_b$) = 2500 psi

Initial Reservoir Temperature = 180^{o}F

Initial Oil in Place (N) = 56000000 STB

Initial Water Saturation (S_{wi}) = 0.2

Initial Oil Saturation (S_{oi}) = 0.8

Table 3.1 gives the fluid property data whereas table 3.2 provides the relative permeability data for the reservoir. Figure 3.1 shows a prepared plot of relative permeabilities to gas and oil versus gas saturation. Power regression has been used to fit a curve to the gas relative permeability and the equation and correlation of the fit is provided. Similarly, exponential regression has been used to fit a line for the oil relative permeability and the equation and correlation of the fit is also provided. These equations are used to determine the relative permeability at specific gas saturations.

This application of the Muskat's method in predicting oil recovery illustrates the proposed procedure by Craft et al, 1991 for solving Muskat's equation fro a given pressure drop Δp, that is, $(p^* - p)$.

Table 3.1: Fluid property data

Pressure	B_o	R_{so}	B_g	U_o	U_g
(psia)	bbl/STB	SCF/STB	bbl/SCF	cp	Cp
2500	1.498	721	0.001048	0.488	0.0170
2300	1.463	669	0.001155	0.539	0.0166
2100	1.429	617	0.001280	0.595	0.0162
1900	1.395	565	0.001440	0.658	0.0158
1700	1.361	513	0.001634	0.726	0.0154
1500	1.327	461	0.001884	0.802	0.0150
1300	1.292	409	0.002206	0.887	0.0146
1100	1.258	357	0.002654	0.982	0.0142
900	1.224	305	0.003300	1.085	0.0138
700	1.190	253	0.004315	1.199	0.0134
500	1.156	201	0.006163	1.324	0.0130
300	1.121	149	0.010469	1.464	0.0126

100	1.087	97	0.032032	1.617	0.0122

Table 3.2: Relative permeability data for the reservoir

Prepared plot of relative permeabilities versus gas saturation

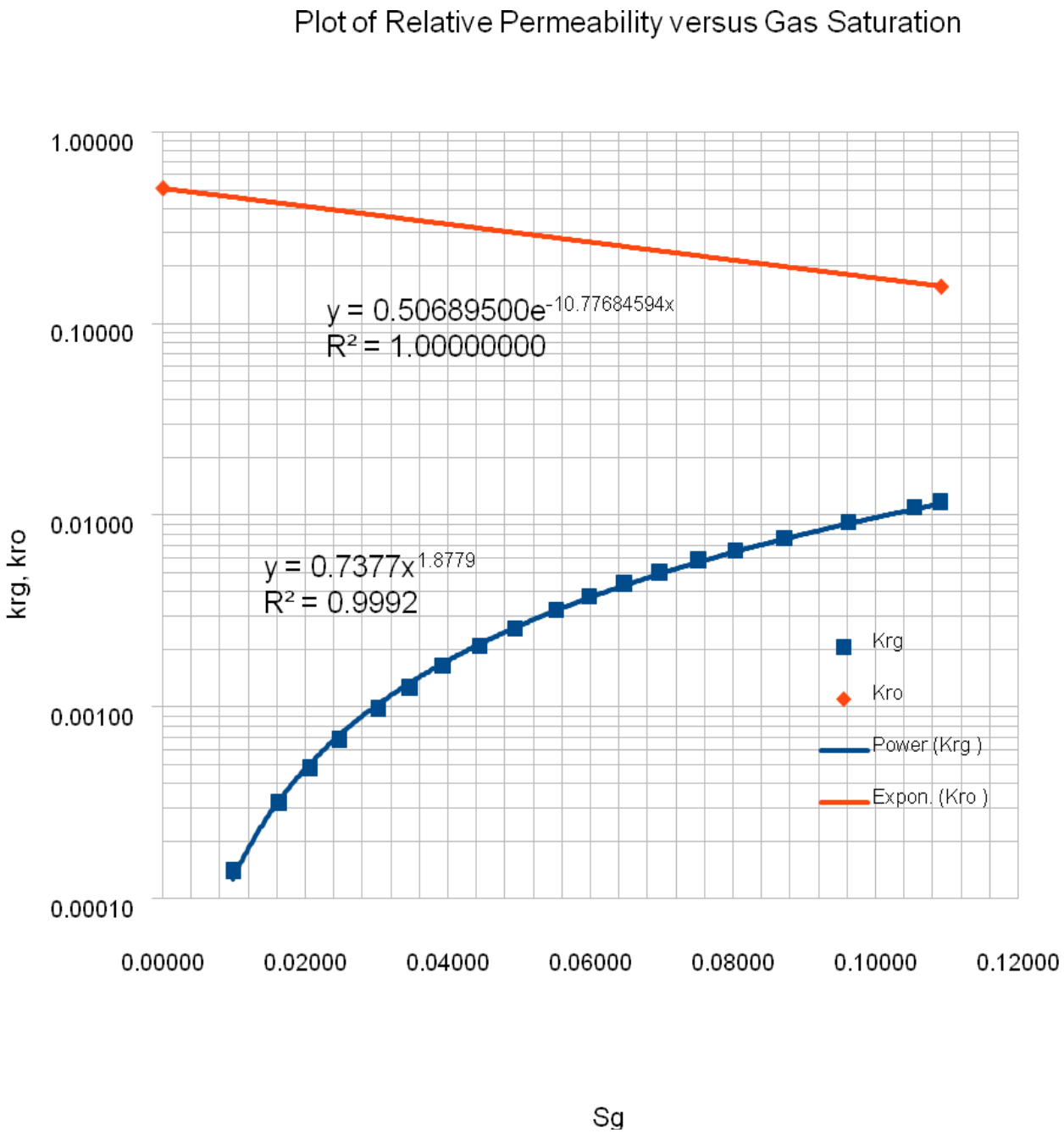

Figure 3.1: Relative permeability plot for the reservoir

Plot R_s, B_o and $(1/B_g)$ versus pressure

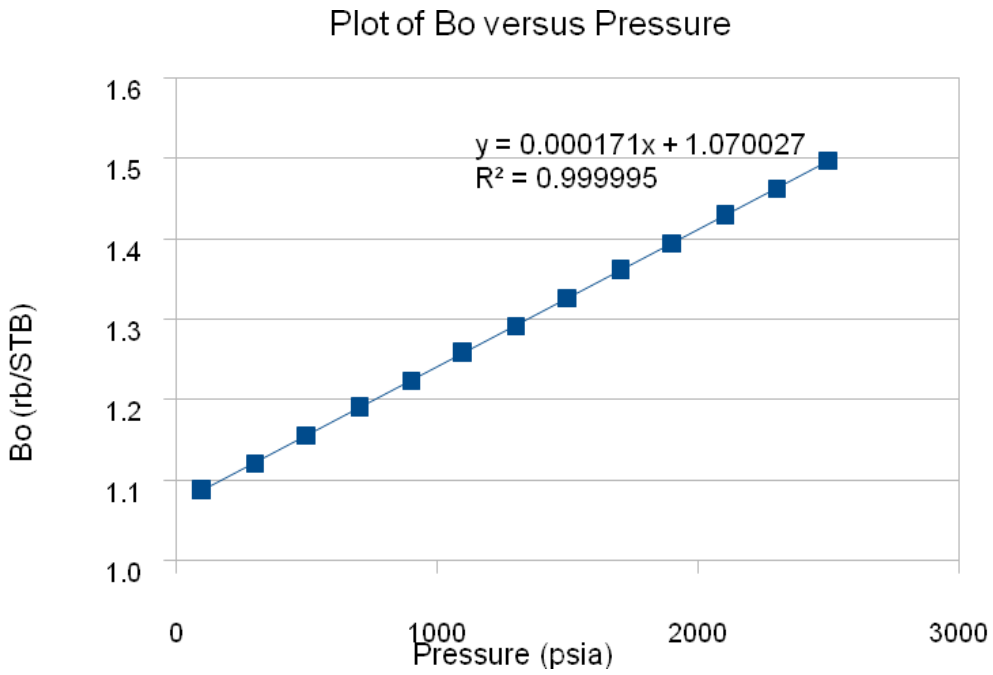

Figure 3.2: Plot of B_o versus pressure

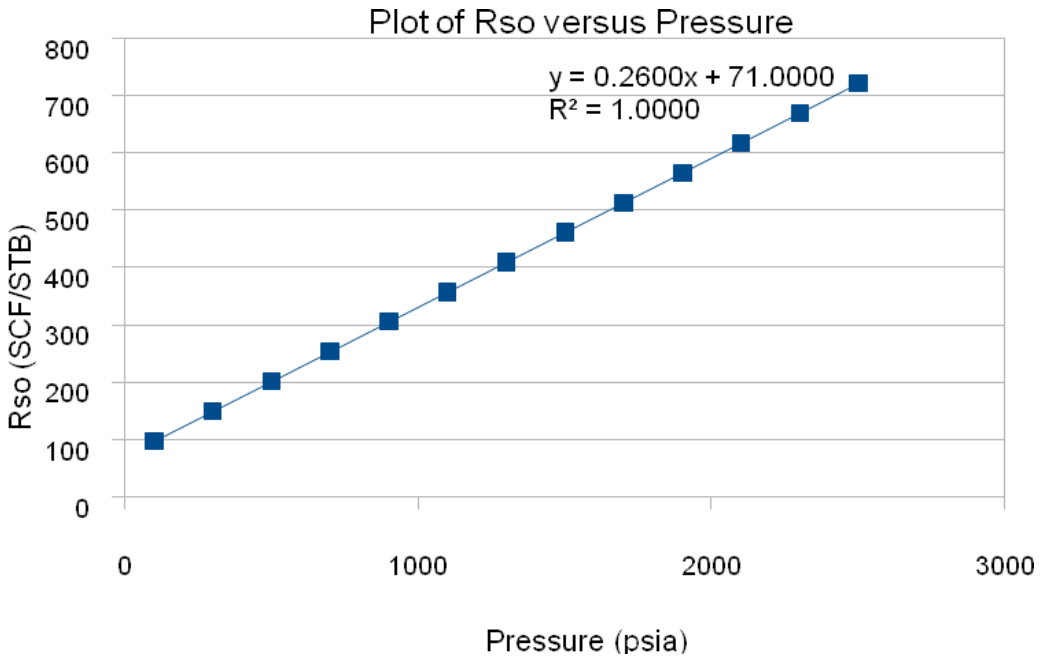

Figure 3.3: Plot of R_{so} versus pressure

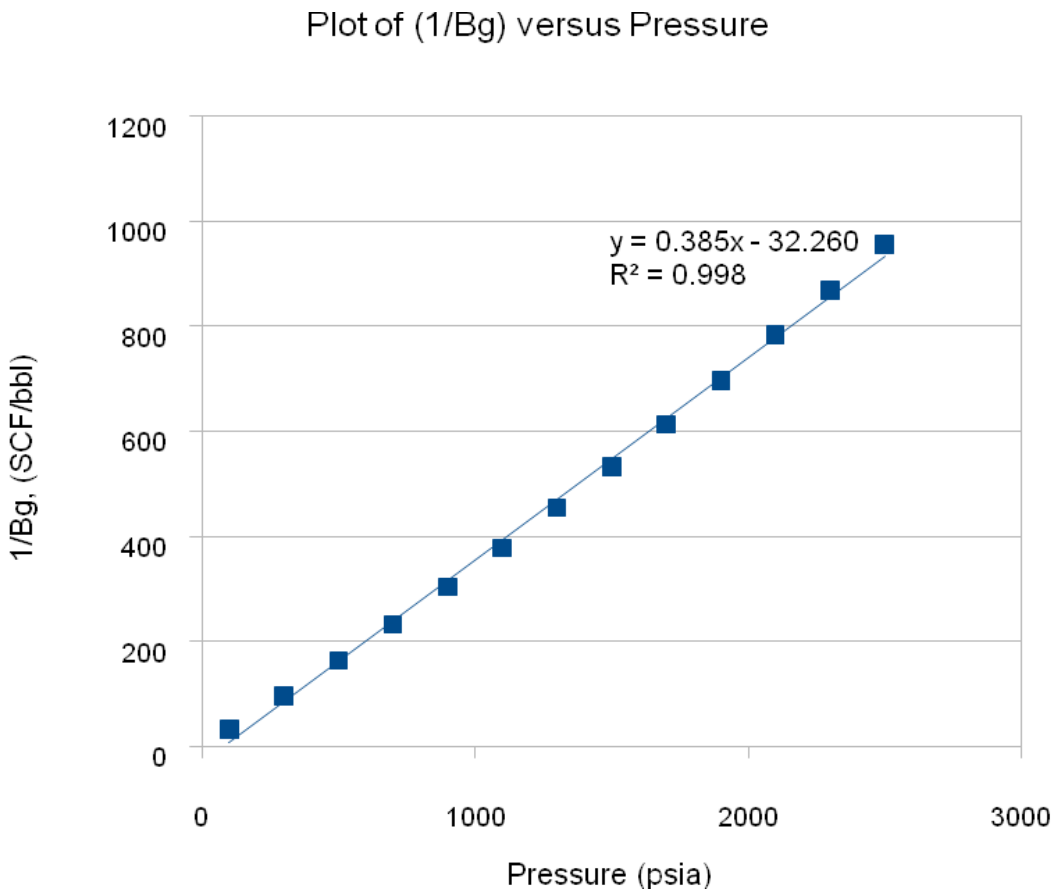

Figure 3.4: Plot of $1/B_g$ versus pressure

Slopes:

$$\frac{dB_o}{dp} = 0.000171 \qquad \frac{dR_{so}}{dp} = 0.26 \qquad \frac{d\left(1/B_g\right)}{dp} = 0.385$$

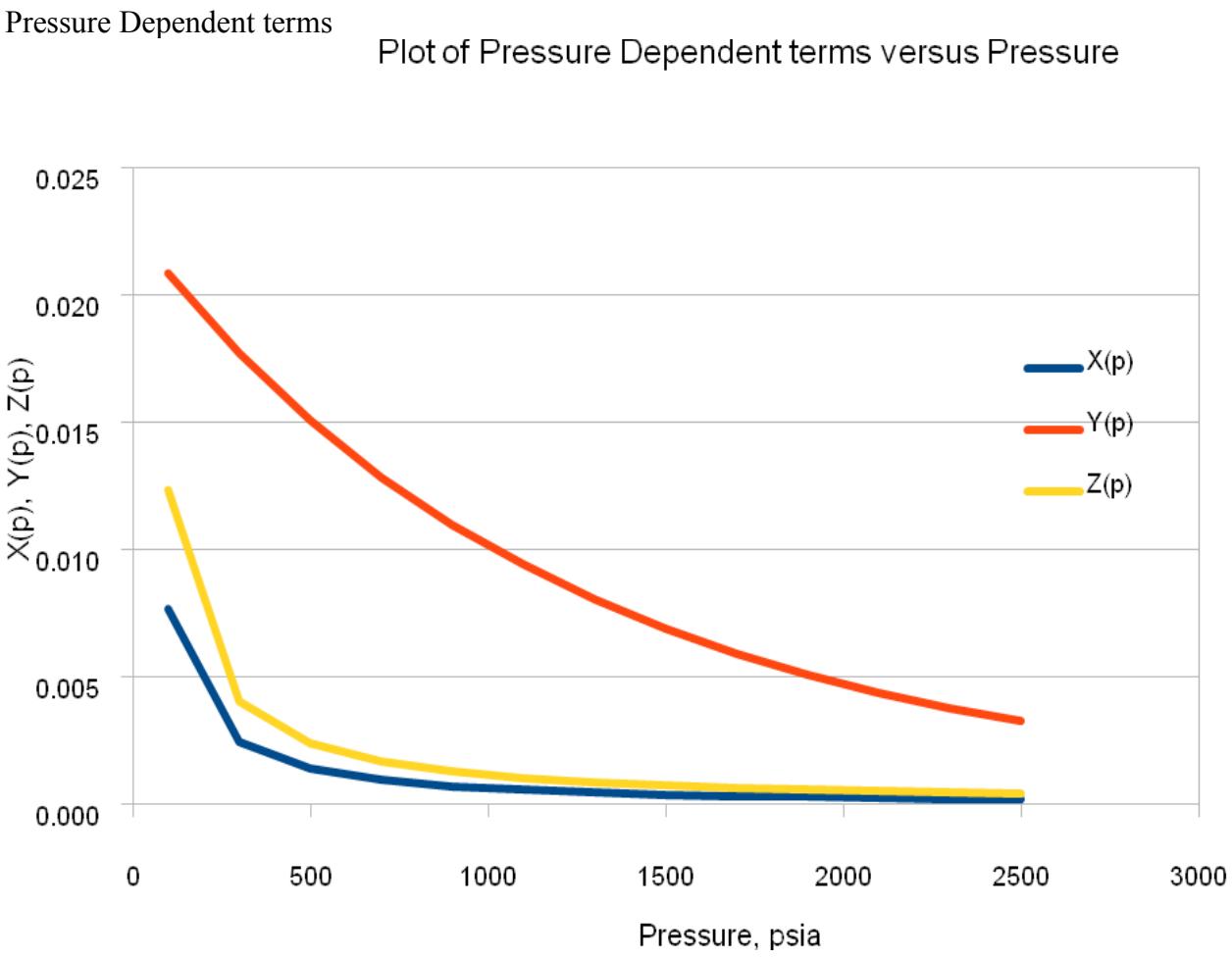

Figure 3.5: Pressure dependent terms as functions of pressure

Table 3.3 (a): Muskat's primary recovery prediction result

Pressure	Bo	Rso	Bg	(1/Bg)	Uo	Ug	Uo/Ug	X(p)	Y(p)	Z(p)
(psia)	bbl/STB	SCF/STB	bbl/SCF	SCF/bbl	cp	cp				
2500	1.498	721	0.001048	954.20	0.488	0.0170	28.70588	0.000182	0.003277	0.000403
2300	1.463	669	0.001155	865.80	0.539	0.0166	32.46988	0.000205	0.003795	0.000445
2100	1.429	617	0.001280	781.25	0.595	0.0162	36.7284	0.000233	0.004395	0.000493
1900	1.395	565	0.001440	694.44	0.658	0.0158	41.64557	0.000268	0.005105	0.000554
1700	1.361	513	0.001634	612.00	0.726	0.0154	47.14286	0.000312	0.005923	0.000629
1500	1.327	461	0.001884	530.79	0.802	0.0150	53.46667	0.000369	0.006890	0.000725
1300	1.292	409	0.002206	453.31	0.887	0.0146	60.75342	0.000444	0.008041	0.000849
1100	1.258	357	0.002654	376.79	0.982	0.0142	69.15493	0.000549	0.009400	0.001022
900	1.224	305	0.003300	303.03	1.085	0.0138	78.62319	0.000701	0.010984	0.001271
700	1.190	253	0.004315	231.75	1.199	0.0134	89.47761	0.000943	0.012858	0.001661
500	1.156	201	0.006163	162.26	1.324	0.0130	101.8462	0.001386	0.015065	0.002373
300	1.121	149	0.010469	95.52	1.464	0.0126	116.1905	0.002428	0.017724	0.004031
100	1.087	97	0.032032	31.22	1.617	0.0122	132.541	0.007662	0.020851	0.012332

Table 3.3 (b): Muskat's primary recovery prediction result continued

Sg*	Krg	kro	krg/kro	Δso/Δp	So	Δso/Δp recalculated	(Δso/Δp) avg	So*
0.0000	0.0000000	0.506895	0.00000					0.8
0.0291	0.0009623	0.370430	0.00260	0.000146	0.7709	0.000165	0.000155	0.7690
0.0310	0.0010860	0.362784	0.00299	0.000165	0.7359	0.000192	0.000178	0.7333
0.0667	0.0045711	0.246958	0.01851	0.000192	0.6948	0.000175	0.000184	0.6965
0.1035	0.0104191	0.166200	0.06269	0.000175	0.6615	0.000136	0.000156	0.6654
0.1346	0.0170778	0.118812	0.14374	0.000136	0.6381	0.000113	0.000125	0.6404
0.1596	0.0235097	0.090773	0.25900	0.000114	0.6177	0.000103	0.000108	0.6188
0.1812	0.0298402	0.071916	0.41493	0.000103	0.5983	0.000097	0.000100	0.5989
0.2011	0.0362961	0.058023	0.62555	0.000097	0.5795	0.000093	0.000095	0.5799
0.2201	0.0429892	0.047296	0.90894	0.000093	0.5613	0.000091	0.000092	0.5615
0.2385	0.0499849	0.038789	1.28863	0.000091	0.5433	0.000090	0.000091	0.5434
0.2566	0.0573459	0.031915	1.79685	0.000090	0.5254	0.000091	0.000091	0.5253
0.2747	0.0651855	0.026253	2.48293	0.000091	0.5071	0.000102	0.000097	0.5060

Table 3.3 (c): Muskat's primary recovery prediction result continued

Np (STB)	GOR (scf/STB)	Gp (scf)	Np/N	Recovery (% STOIIP)
	721		0.0000	0
8.85E+005	775.8450591	6.62E+008	0.0158	1.580
2.19E+006	739.7453027	1.65E+009	0.0391	3.915
3.64E+006	1311.755505	3.14E+009	0.0651	6.506
4.73E+006	2974.617372	5.48E+009	0.0846	8.455
5.40E+006	5874.083304	8.40E+009	0.0963	9.634
5.78E+006	9624.532692	1.14E+010	0.1032	10.318
6.08E+006	13958.2386	1.49E+010	0.1086	10.859
6.32E+006	18547.31895	1.88E+010	0.1128	11.285
6.52E+006	22682.3057	2.30E+010	0.1165	11.645
6.71E+006	24818.28543	2.74E+010	0.1198	11.979
6.86E+006	22504.40129	3.11E+010	0.1226	12.257
7.19E+006	11264.60316	3.66E+010	0.1284	12.843

Plots from result of Muskat's oil recovery prediction

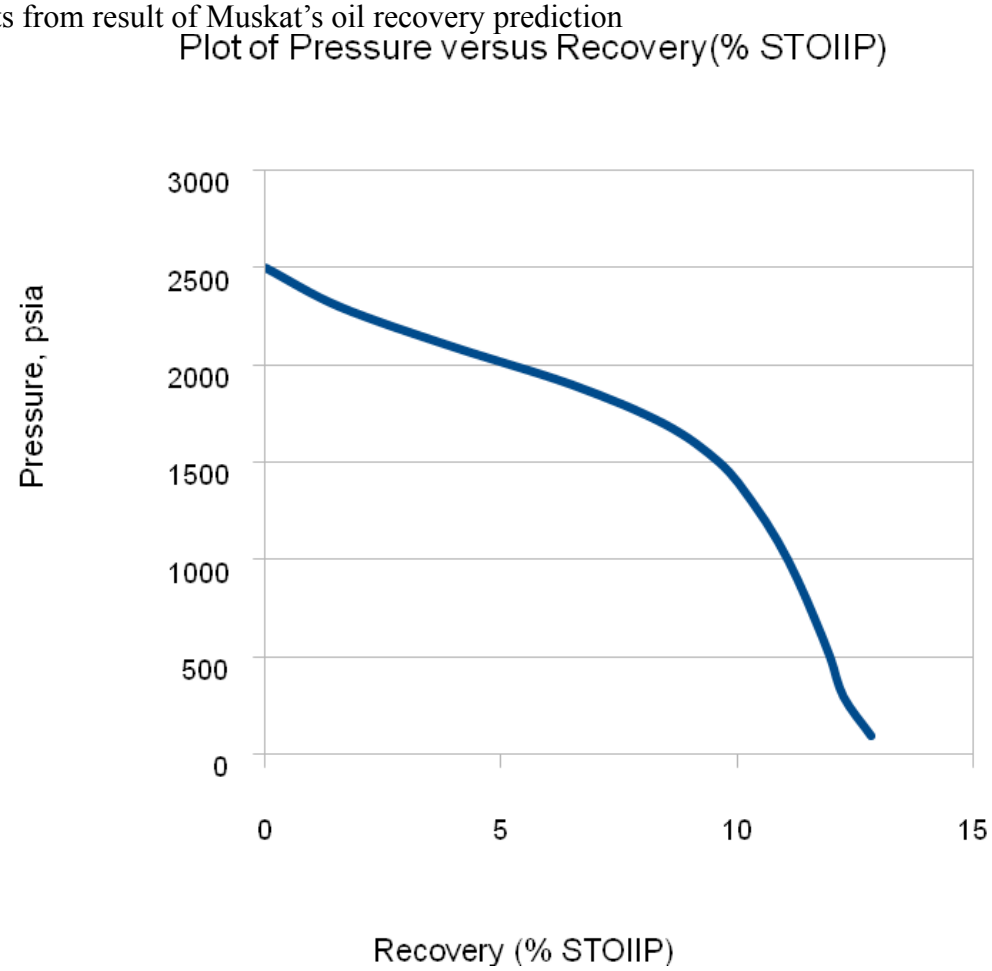

Figure 3.6: Pressure decline as a function of the oil recovery

It is observed from figure 3.6 that a recovery of about 13% STOIIP only could be obtained at a depletion pressure of 100 psi (abondonement). This depicts a typical final recovery factor in this kind of reservoirs (solution – gas drive), ranging approxiamtely from 7 to 35% of the STOIIP (Cosentino, 2001).

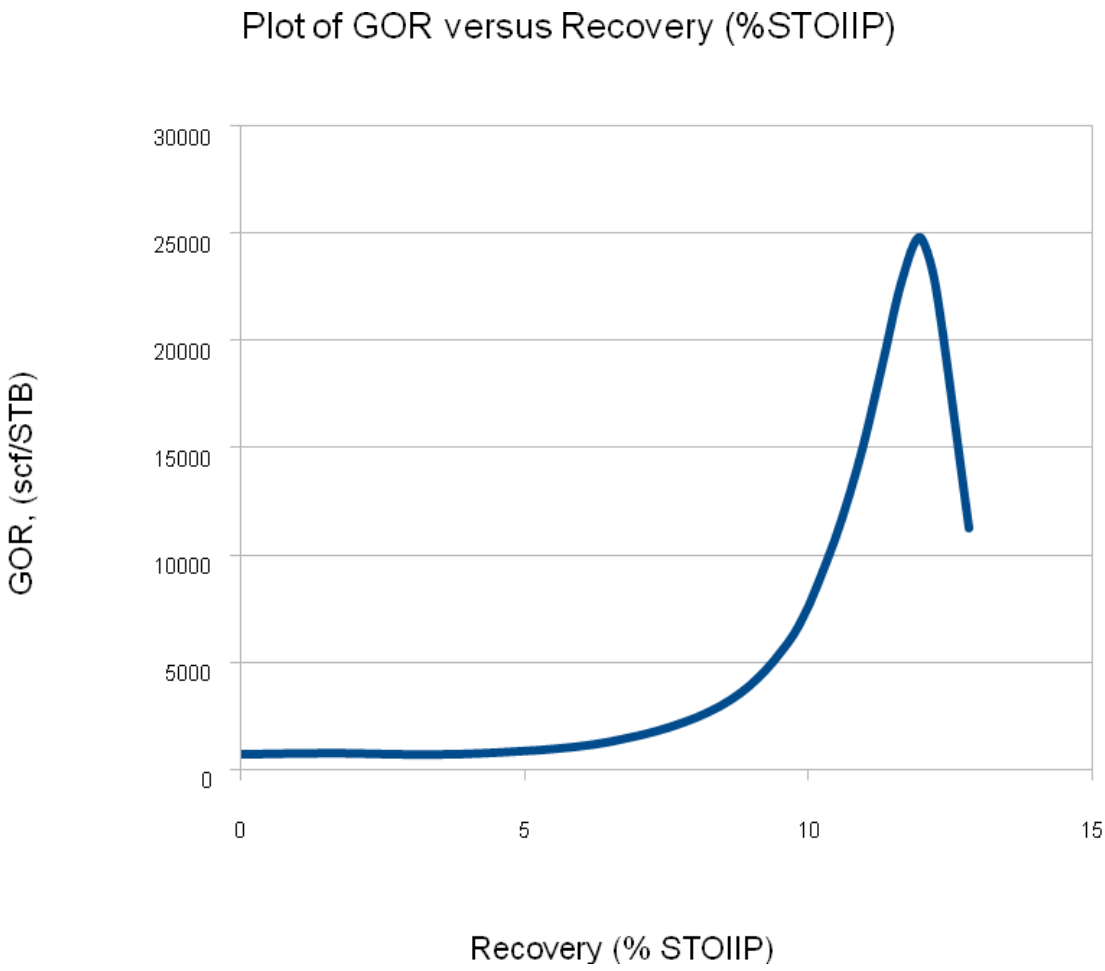

Figure 3.7: GOR development as a function of oil recovery

It is observed from figure 3.7 that a recovery of about 13% STOIIP could be obtained at a GOR of about 12,000 scf/stb.

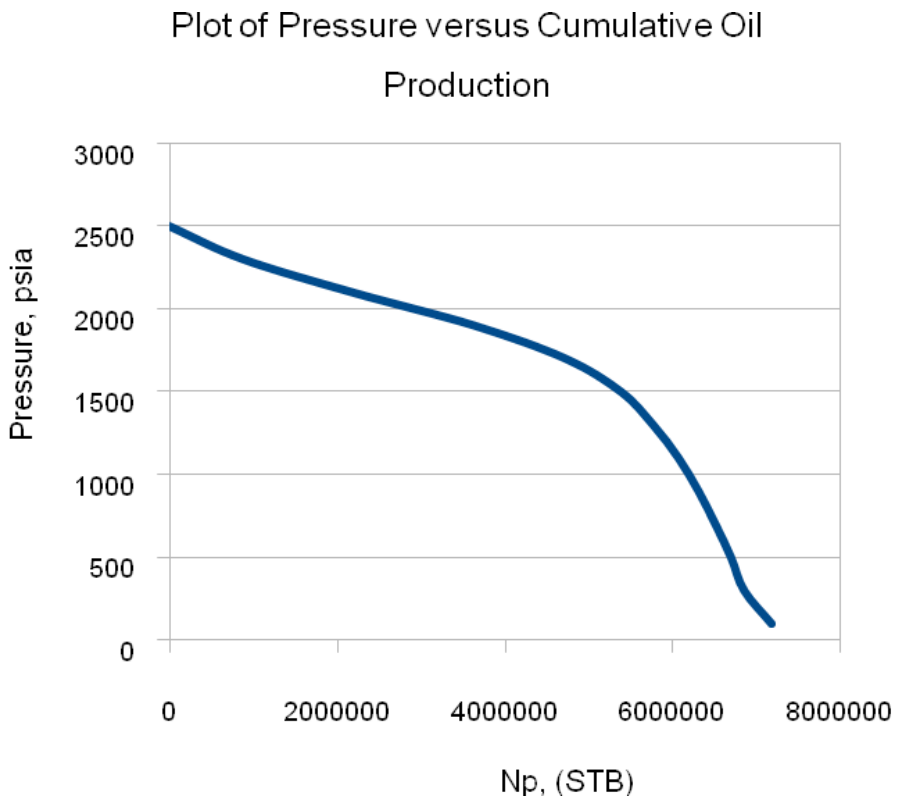

Figure 3.8: Pressure decline as a function of cumulative oil produced

Figure 3.8 exhibits similar behavior as figure 3.6 with a cumulative oil production of about 7.2 MM stb at abondonment pressure.

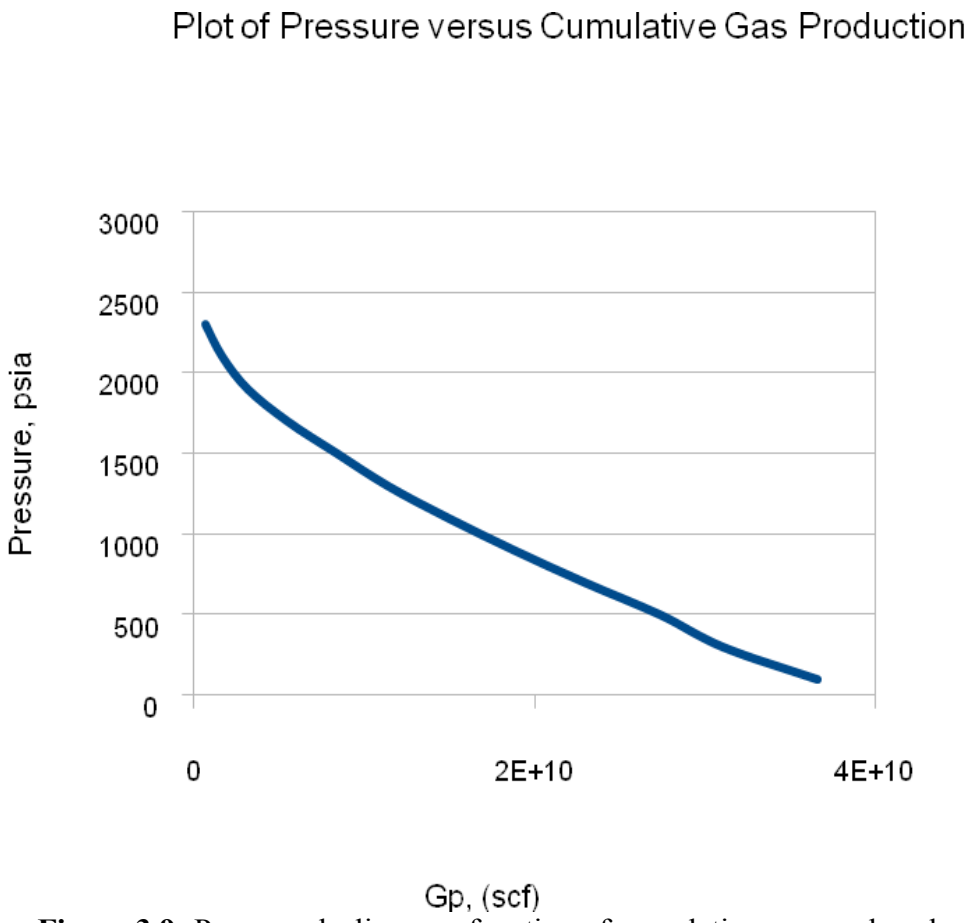

Figure 3.9: Pressure decline as a function of cumulative gas produced

Gas begins to flow when the critical gas saturation is reached. Figure 3.9 shows an inverse relationship which buttresses the fact that, the more the pressure drops, the faster the gas is liberated and produced, thus lowering further the pressure, in a sort of chain reaction that quickly leads to the depletion of the reservoir (Cosentino, 2001).

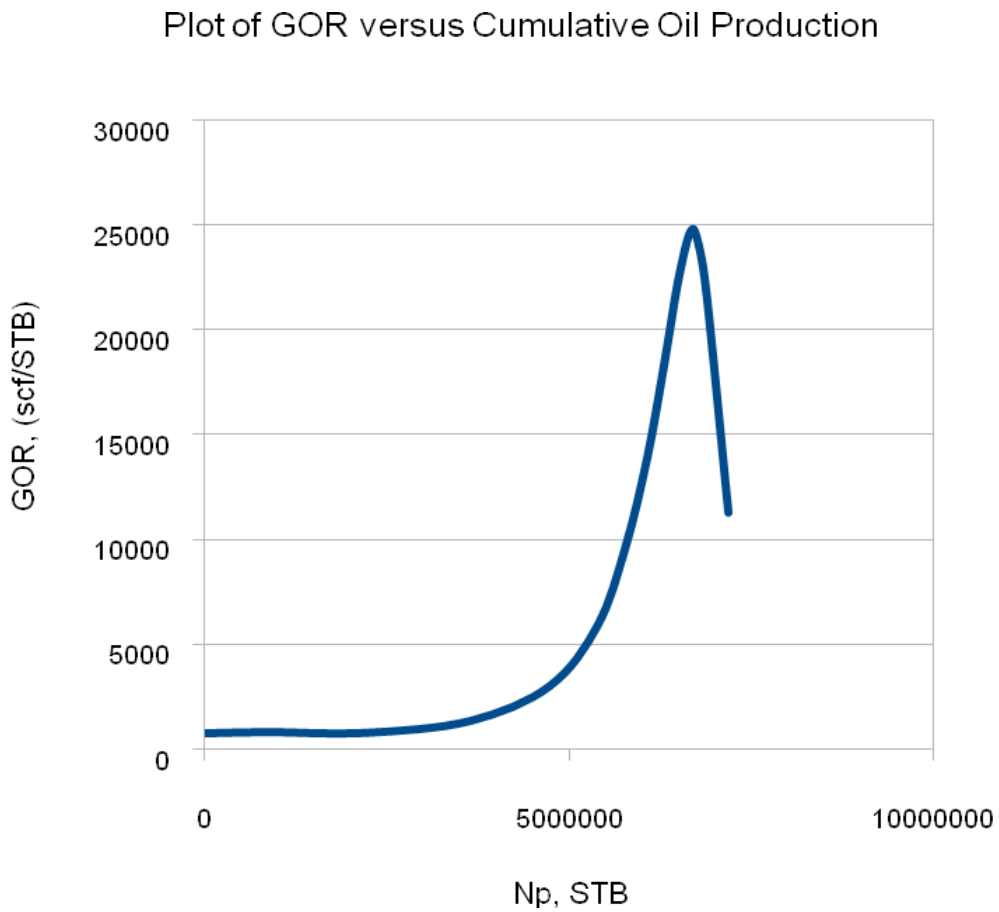

Figure 3.10: GOR development as a function of cumulative oil produced

Figure 3.10 exhibits similar behavior as figure 3.7 with a GOR of about 12,000 scf/stb corresponding to a cumulative oil production of about 7.2 MM stb.

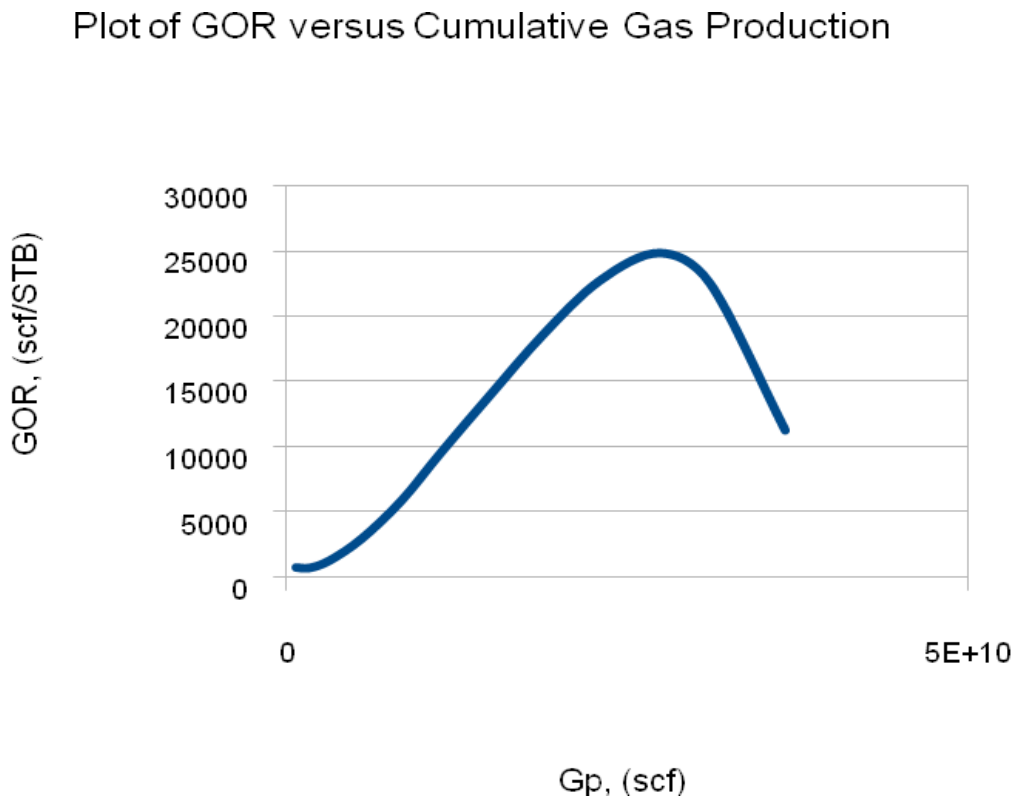

Figure 3.11: GOR development as a function of cumulative gas produced

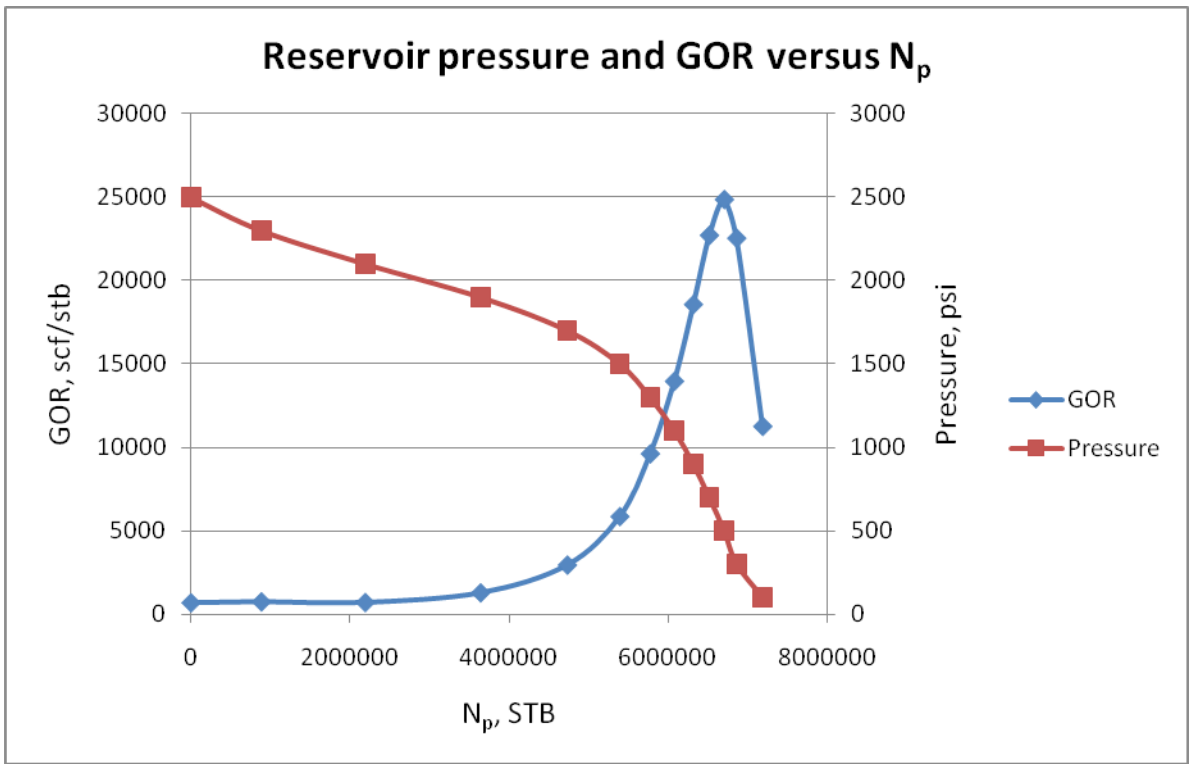

Figure 3.12: Characteristics of the reservoir (solution – gas drive reservoir)

Chapter 4

4.0 Design of Artificial Lift and Tubing Strings

4.1 Determining Feasibility

Figure 4.1 shows a graph of average reservoir pressure as a function of cumulative oil production. The continuous pressure drop results in faster liberation and production of gas, thus lowering further the pressure, in a sort of chain reaction that quickly leads to the depletion of the reservoir as shown in figure 4.1 (Cosentino, 2001). From figure 4.2, it is observed that a recovery of only about 13% of STOIIP could be obtained at a depletion pressure of 100 psi (abandonment pressure) when the reservoir is depleted naturally. Such low recovery prompts the use of artificial lift design (gas lift design) for the reservoir in order to optimize production and maximize return on investment.

In addition, since the reservoir exists originally at its bubble point, critical gas saturation may be reached very early which may result in the production of appreciable quantity of gas at an early stage of depletion. This gas can be made available for injection back into the reservoir to gas lift the well. Hence, the need for gas lifts design.

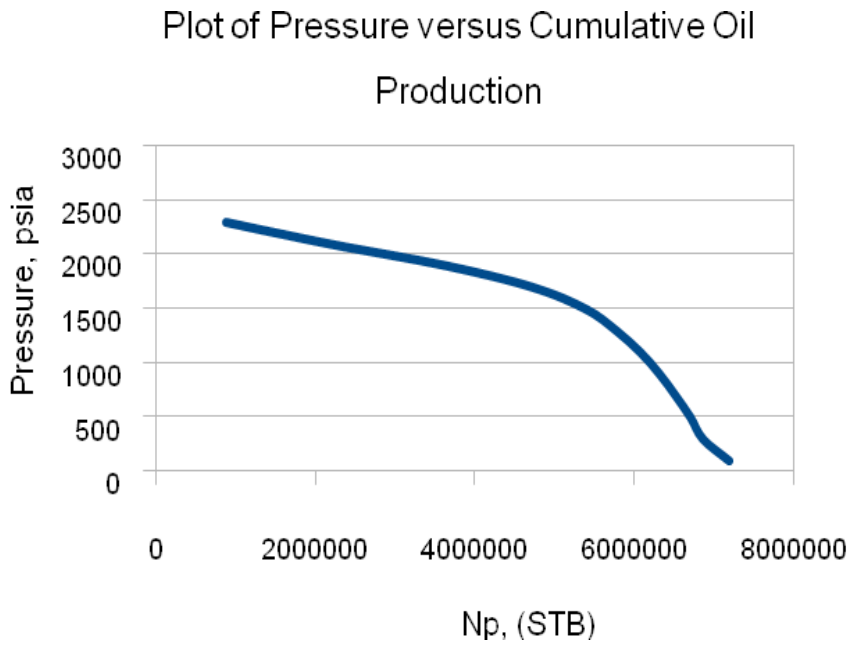

Figure 4.1: Average reservoir pressure as a function of cumulative oil production

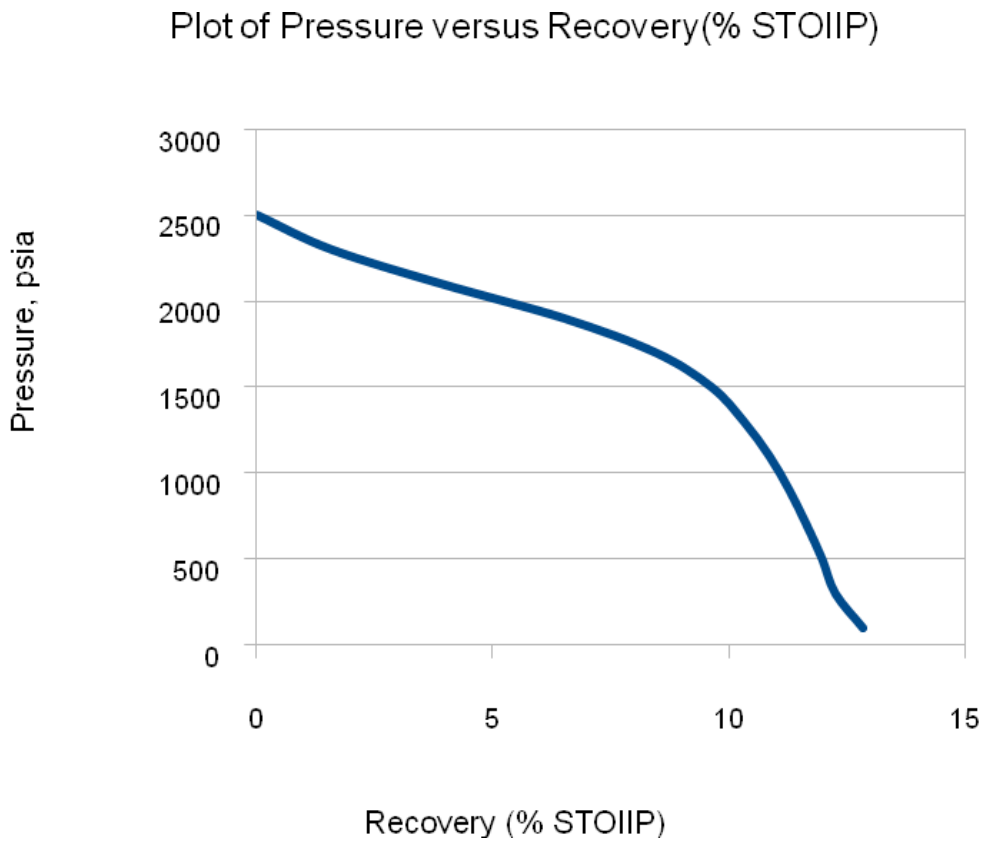

Figure 4.2: Average reservoir pressure decline as a function of recovery

4.2 Design Data/Parameters

The following data is available for the oil well:

Average reservoir pressure = 2500 psi

Water Cut = 0%

Initial Gas – Liquid ratio (GLR_i) = 721 scf/stb

J^* = 1.5

API = 25

Specific gravity to gas = 0.7

Average Temperature = 180 ^oF

Reservoir depth = 7500 ft

Wellhead pressure = 150 psi

Inclination angle with Horizontal = 90^o (vertical well)

Nominal tubing sizes of 1/2”, 1”, 1 1/2”, 2 3/8”, or 3 ½” is employed in the design of the gas lift.

4.3 Inflow Performance Relationship (IPR)

Since the reservoir originally exists at its bubble point pressure, fluid flowing in the reservoir goes to multiphase conditions immediately at the start of production when the pressure is lower than the bubble point. This means the linear IPR (see Appendix B) will not be valid (since saturated). As the pressure inside the reservoir goes below the bubble point value, gas comes out of solution reducing the oil saturation and relative permeability, and increasing oil viscosity. Also the formation volume factor is always greater than one due to the gas in solution (Prado, 2008). The oil productivity is reduced since now the driving force for fluid movement is spent moving the liquid and the gas phases (Prado, 2008). The constant productivity index (PI) concept is no longer valid. Since IPR under multiphase flow conditions can not be easily calculated, Fetkovich's empirical correlation is employed to estimate the IPR.

4.3.1 Fetkovich's Correlation

Fetkovich's correlation is usually the one that is more conservative always under predicting flow capacity in comparison to the other IPR equations (Prado, 2008). Fetkovich is also a simpler equation which in some cases can simplify some of the calculations. Even being the most conservative of the IPRs, because it is not a model and just a correlation, it can over predict flow capacities for some reservoirs that are severely affected by the presence of free gas in the porous media. Fetkovich's correlation is given by equation 4.1 as:

$$\frac{q}{q_{max}} = 1 + b\left(\frac{P_{wf}}{\overline{P}}\right) - \left|1 + b\left(\frac{P_{wf}}{\overline{P}}\right)^2\right| \qquad (4.1)$$

where

b = 0

At the bubble point pressure (that is $P_b = P_{avg}$), the corresponding bubble point flowrate is given by equation 4.2 as:

$$q_b = J^{¿}\left(\overline{P} - P_b\right) \tag{4.2}$$

$$q_b = 1.5\left(2500 - 2500\right) = 0$$

The absolute open flow (AOF) or the maximum flowrate q_{max} is given by equation 4.3 as:

$$q_{\max} = q_b + \frac{J^{¿} P_b}{2 + b} \tag{4.3}$$

$$q_{\max} = 0 + \frac{1.5 \times 2500}{2} = 1875 \text{ bpd}$$

Figure 4.3 shows the present IPR curve for the reservoir at its initial conditions using Fetkovich.

4.3.2 Beggs and Brill Correlation

The Beggs and Brill program (Prado, 2008) is a spreadsheet program developed to obtain the IPR and OPR curves. The Beggs and Brill correlation enables the calculation of the pressure gradient as a function of other production variables like pipe diameter, GLR and gas and oil flow rates. This correlation considers Slip and flow regime. It is applicable to inclined wells with or without water cut. It also predicts pressure drop for upward and downward fluid flow with accuracy.

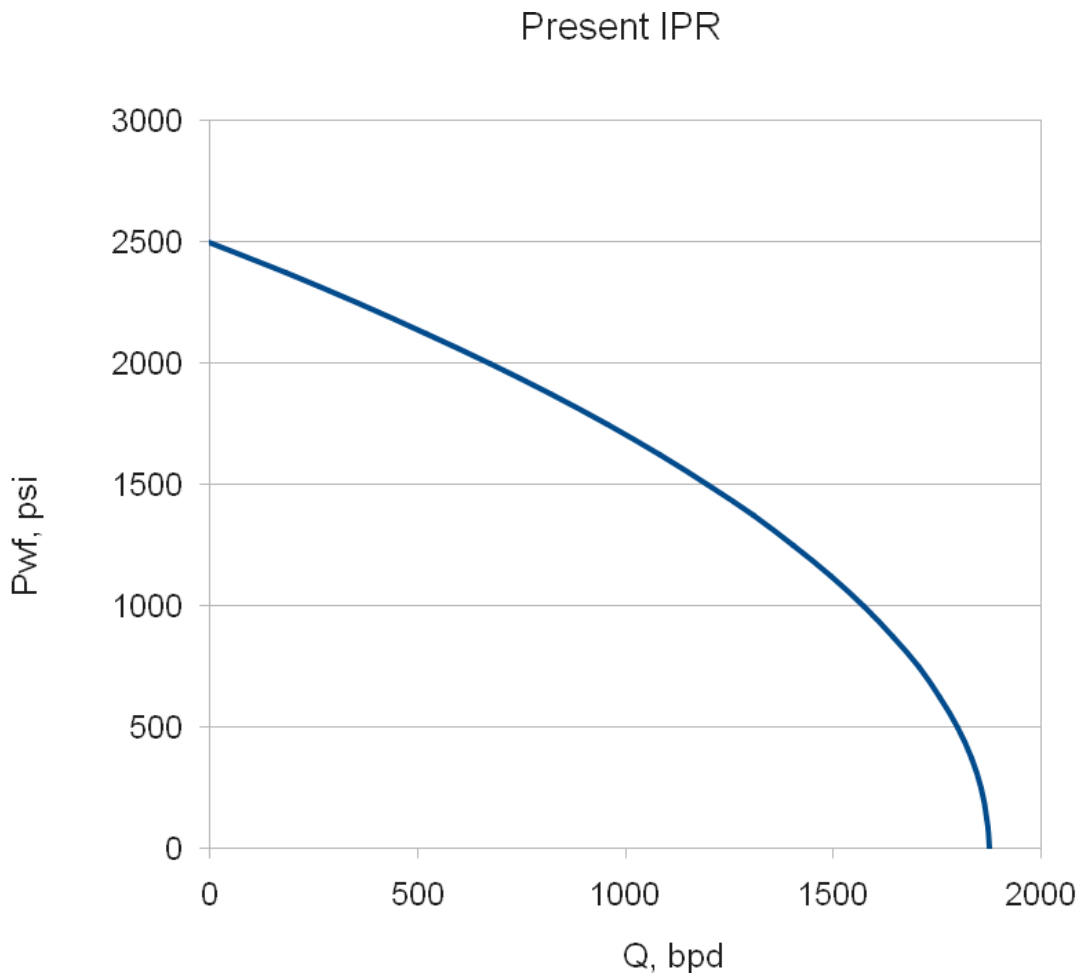

Figure 4.3: Present IPR of reservoir at initial conditions

4.4 Saturated Future IPR

The prediction of the future IPR is very important to forecast future well production. There are many approximate methods to simulate the effects of depletion on productivity index for saturated conditions (Prado, 2008). Usually, those methods provide an equation relating changes in the productivity index J^* as a function of reservoir average pressure. The methods for future reservoir prediction express changes in J^* as a function of changes in average reservoir pressure. One of such methods is the Eickmeier method which is used in this case study.

4.4.1 Eickmeier Method

The Eickmeier method is given by equation 4.4 as:

$$\frac{J^{\bar{P}_2}}{J^{\bar{P}_1}} = \left(\frac{\bar{P}_2}{\bar{P}_1}\right)^2 \qquad (4.4)$$

The effect of changes in average reservoir pressure over the absolute open flow is also determined using equation 4.5 as:

$$\frac{q_{\max}^{\bar{P}_2}}{q_{\max}} = \left(\frac{\bar{P}_2}{\bar{P}_1}\right)^3 \qquad (4.5)$$

Figure 4.4 shows saturated future IPR curves at selected depletion pressures.

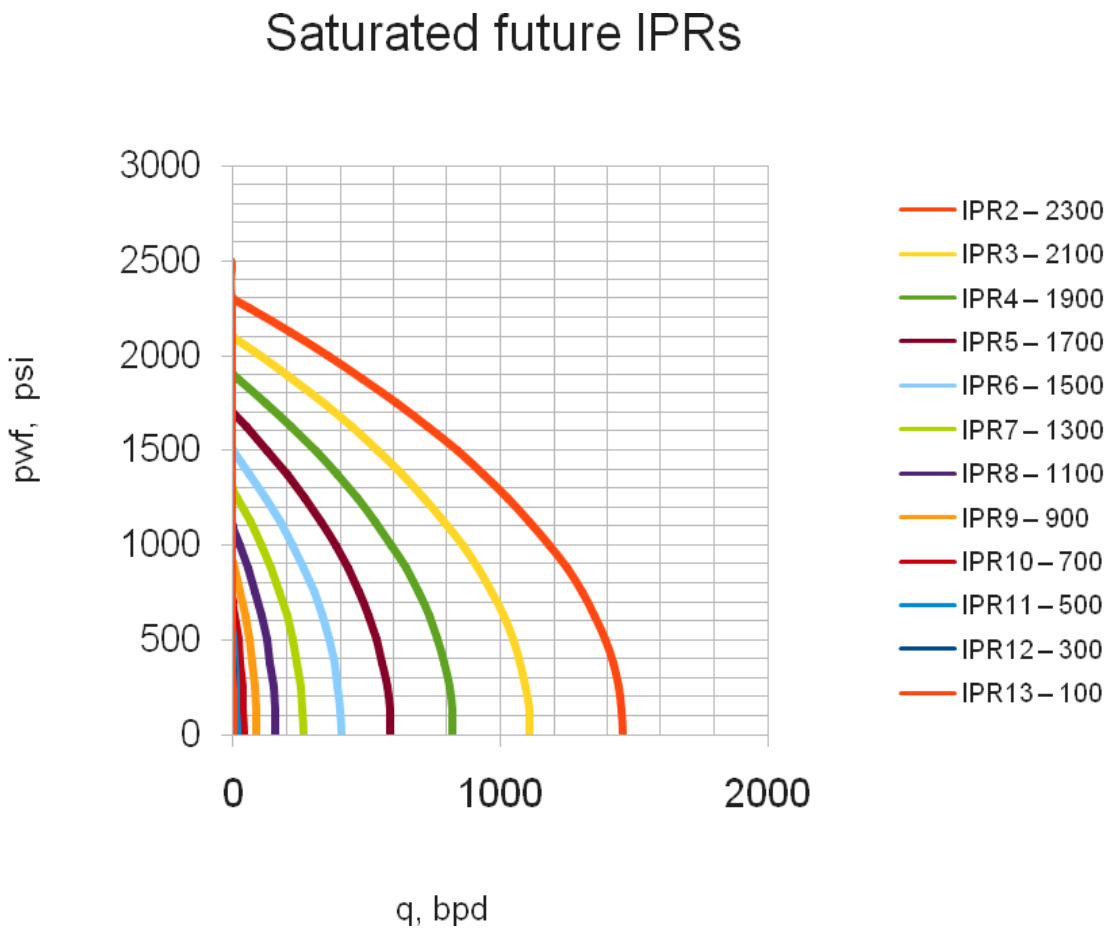

Figure 4.4: Saturated future IPRs using Eickmeier method

4.5 Tubing String Design and Selection

The size (diameter) of the production tubing can play an important role in the effectiveness with which the well can produce liquid (Lea et al., 2008). There is an

optimum tubing size for any well system (Beggs, 2003). Smaller tubing sizes have higer frictional losses and higher gas velocities which provide better transport for the produced liquids. Larger tubing sizes, on the other hand, tend to have lower frictional pressure drops due to lower gas velocities and in turn lower the liquid carrying capacity (Lea et al., 2008). Tubing too large will cause a well to load up with liquids and die (Beggs, 2003). In designing tubing string, it then becomes important to balance these effects over the life of the field (Lea et al., 2008). Figure 4.5 is a plot of the outflow performance (OPR) of the various tubing sizes superimposed on the IPR curves. It is clearly observed that the smaller size tubings (0.5", 1" and 1.5") have excessive frictional losses with low production rates thereby restricting production. For this reason, only the three larger size tubings (2 3/8", 2 7/8" and 3 ½") are considered to be the better candidates to start producing the well. However, the 3 ½" tubing exhibits the lowest frictional loss which might cause the well to load up with liquids and die too early. The 2 7/8" tubing gives a much more reasonable frictional loss as compared to that of 3 ½" and 2 3/8" tubings with an equilibrium production rate of about 1350 bpd and an equivalent bottomhole flowing pressure of about 1350 psi (figure 4.6).

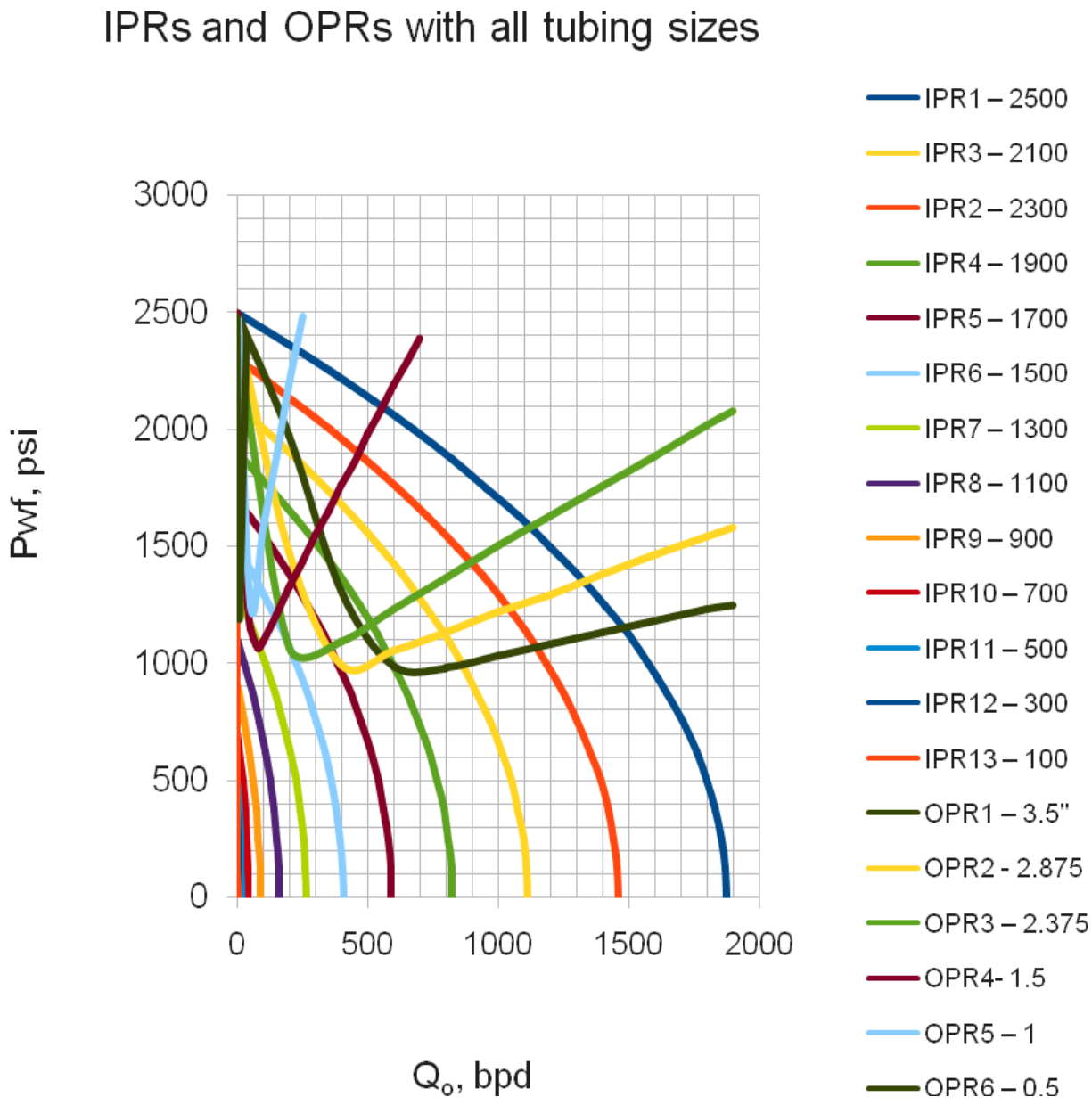

Figure 4.5: Plot of IPRs and OPRs for the various tubing sizes

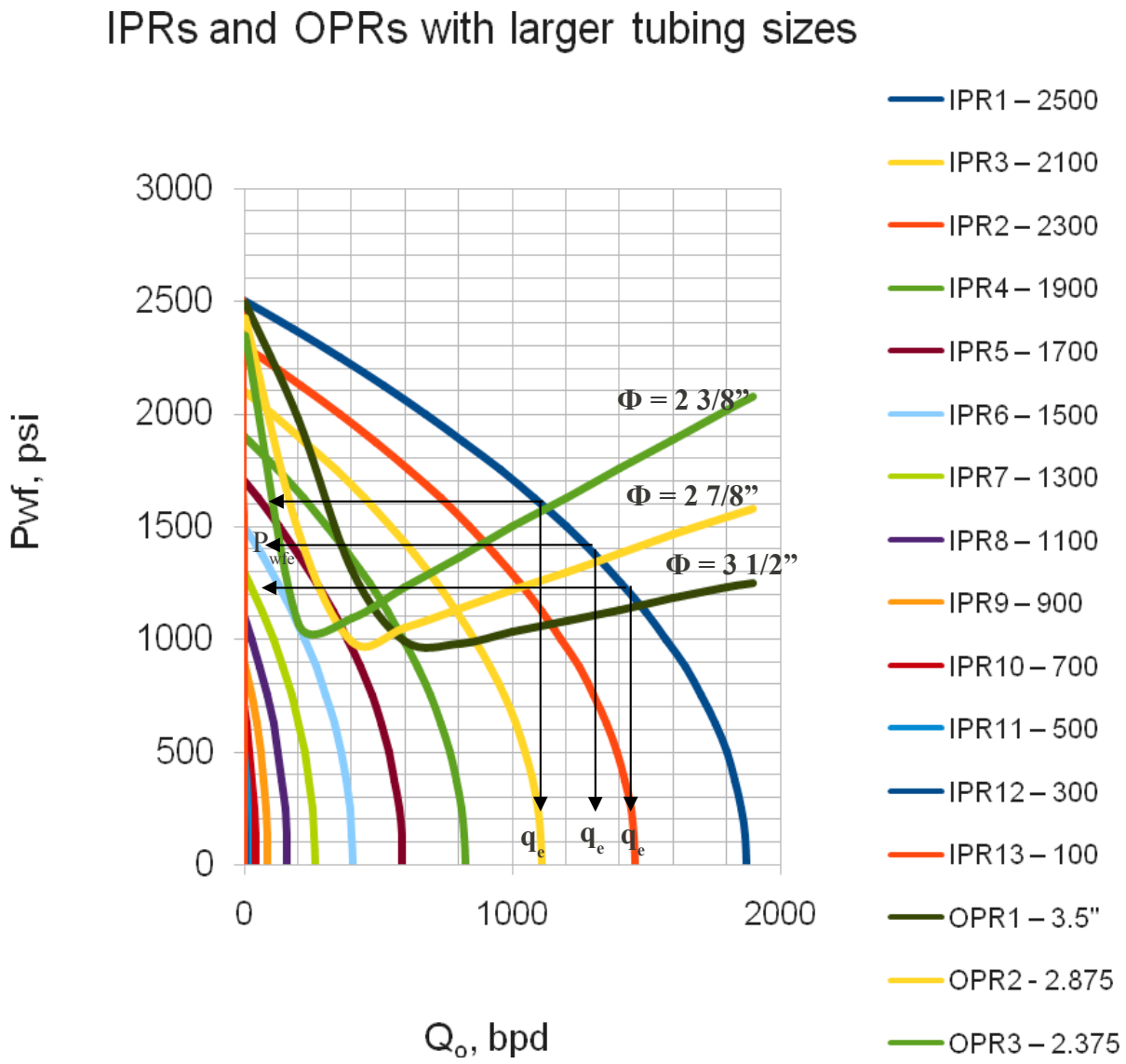

Figure 4.6: OPRs of larger tubing sizes and IPRs

The flow capacities for the various tubing sizes are read from the intersections of the inflow and outflow curves as:

Table 4.1: Equivalent flow capacities of larger tubing sizes

Tubing size, inches	Producing Capacity, bpd
2 3/8	1100
2 7/8	1350
3 1/2	1480

Since the effect of gravity (dominant at lower flowrate areas) is observed at almost a common bottomhole flowing pressure point, that is P_{wf} of about 1000 psi for the three different tubing sizes, its suggests that the effect of gravity is the same irrespective of the tubing size selected. However, this is not the case for the frictional loss effect (dominant at higher flowrate areas). The 2 7/8" tubing produces the reservoir from an average pressure of 2500 psi at a GOR of 721 scf/stb up to a pressure of about 1700 psi as shown in figure 4.7.

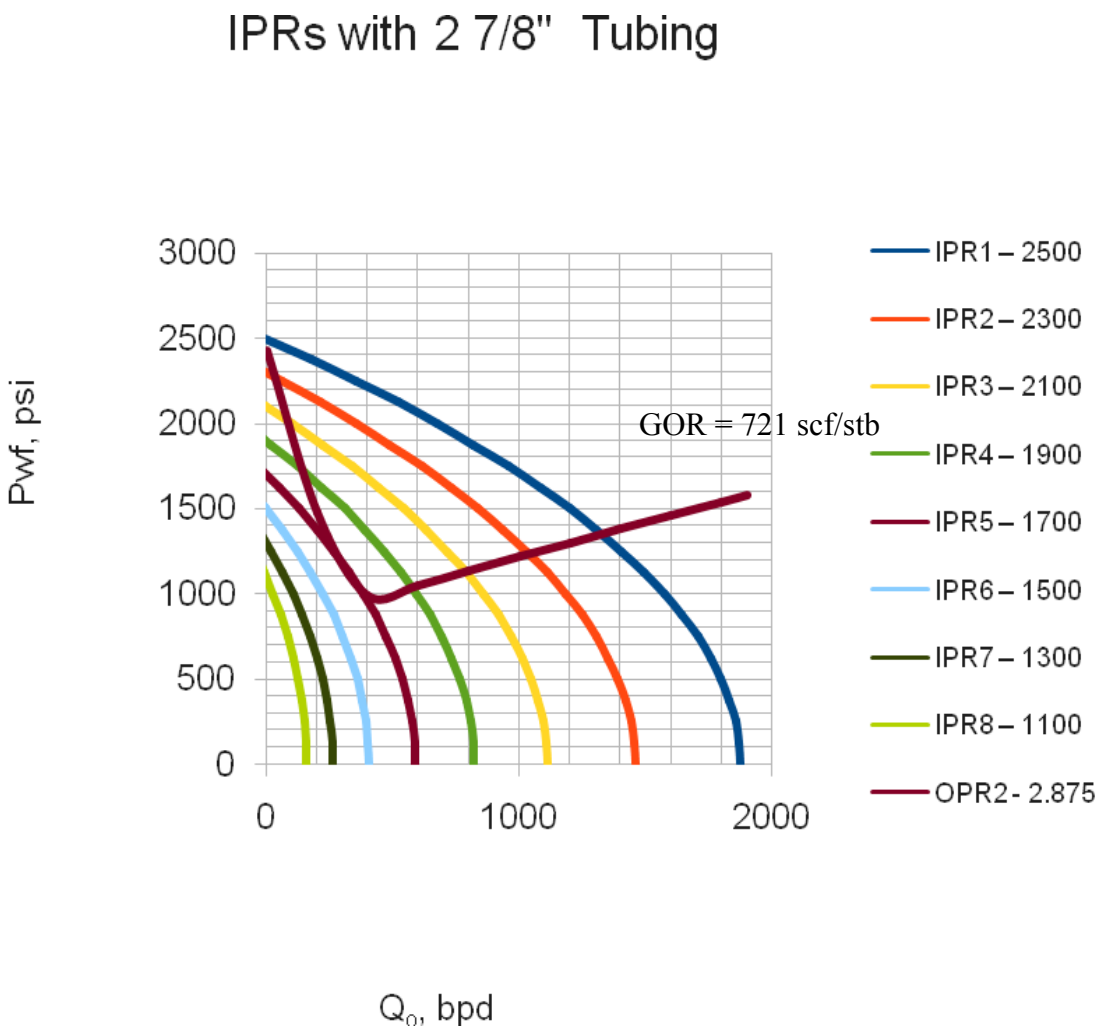

Figure 4.7: Performance of 2 7/8" tubing

4.6 Larger Tubings with Gas Lift

The performances of the 2 7/8" and 2 3/8" tubings are investigated with increase in the GOR. Varying GORs of 1000, 1500, 2000 and 2500 scf/stb are analysed and plotted as shown in figures 4.8 and 4.9.

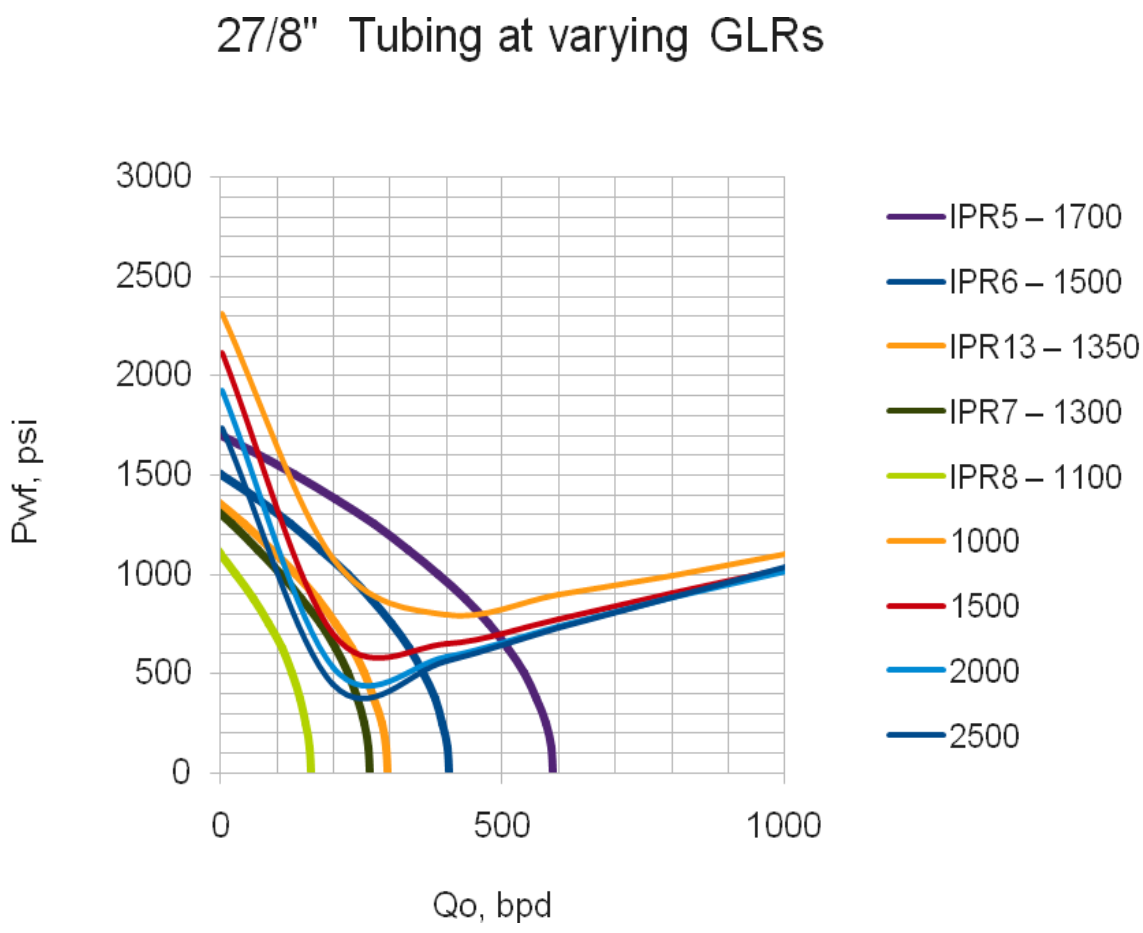

Figure 4.8: Performance of 2 7/8" tubing with varying GORs

From figure 4.8, it is observed that GLRs of 2000 and 2500 virtually give almost the same flow capacities of 500 bpd and equivalent bottomhole flowing pressure of 650 psi. This may be as a result of the gas saturation reaching its critical point. In addition, higher frictional loss is observed at higher flowrates for the two GORs. GLR of 1500 exhibits reasonable frictional loss with an equivalent flowrate of about 500 bpd (same with 2000 and 2500 GORs) and an equivalent bottomhole flowing pressure of 700 psi. GLR of 1000 shows frictional loss same as that of 1500 GOR but can only produce the reservoir to a pressure of 1500 psi ($\Delta p = 200$).

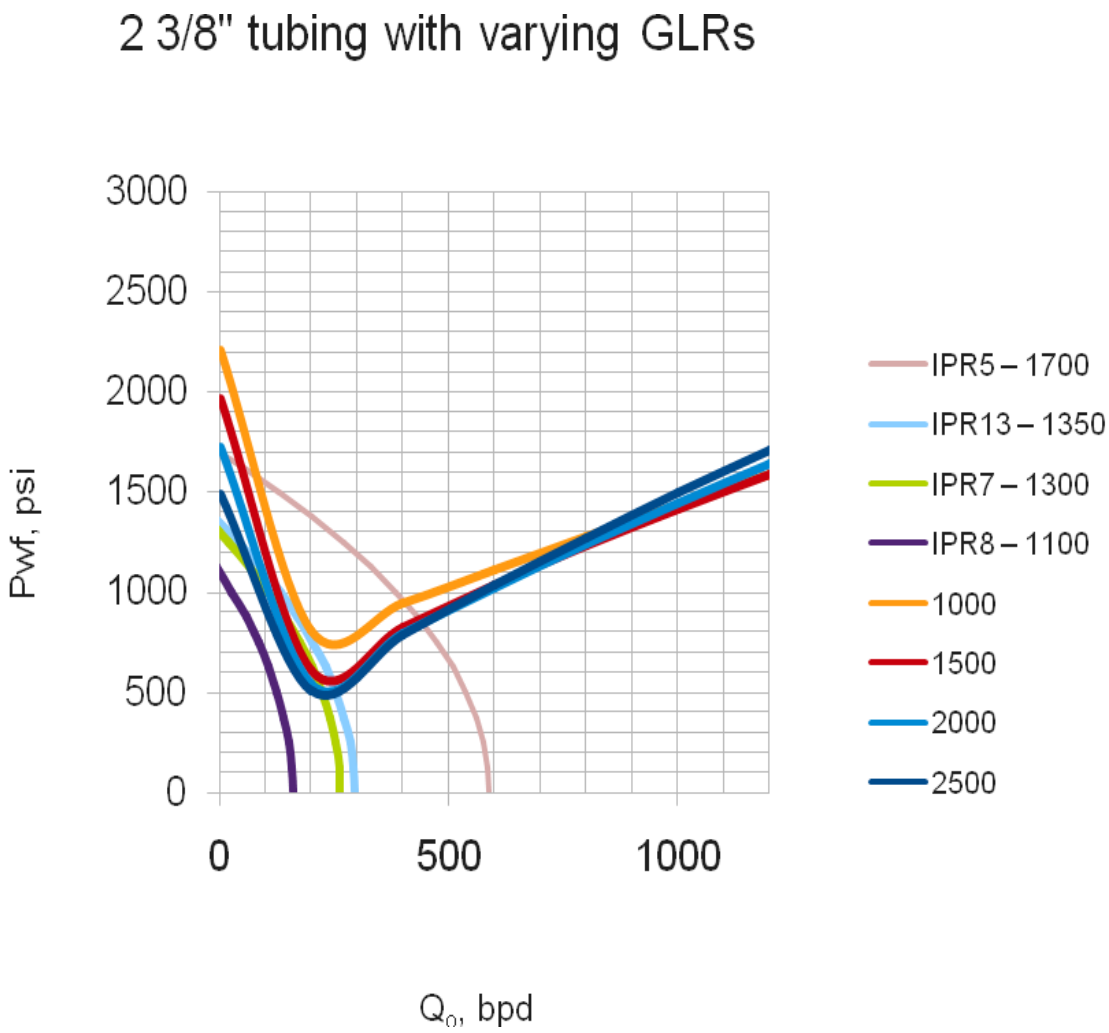

Figure 4.9: Performance of 2 3/8" tubing with varying GORs

From figure 4.9, it is observed that GLRs of 2000 and 2500 give almost the same flow capacities of 450 bpd and equivalent bottomhole flowing pressure of 850 psi. In addition, higher frictional loss is observed at higher flowrates for the two GORs. GLR of 1500 exhibits reasonable frictional loss with an equivalent flowrate of about 450 bpd (same with 2000 and 2500 GORs) and an equivalent bottomhole flowing pressure of 900 psi. GLR of 1000 shows frictional loss lower than that of 1500 GOR but cannot produce the reservoir to a pressure of 1500 psi (Δp = 200 psi). Table 4.2 gives a summary of the foregoing analysis.

Table 4.2: Summary of equivalent flow capacity and bottomhole flowing pressures

From the foregoing argument, a gas lift operation with a GOR of 1500 scf/stb on the 2 7/8" tubing proves to be the better choice. The 2 3/8" tubing does not perform any better than the 2 7/8" tubing and removing the already installed 2 7/8" for the 2 3/8" tubing causes time and money to be lost. Therefore, the reservoir is produced using the 2 7/8" tubing with a GOR of 1500 scf/stb from an average reservoir pressure of 1700 psi to 1300 psi.

Producing at lower pressures below 1350 psi with a 2 7/8" or 2 3/8" tubing may not be profitable even with gas lift as shown in figures 4.8 and 4.9. At this later stage in the life of the reservoir, velocity strings (smaller size tubings) are employed.

4.7 Use of Velocity Strings

Figures 4.10, 4.11, and 4.12 show the performances of the velocity strings (tubing sizes of 1.5", 1" and 0.5") under gas lift operations. The investigation is done with GORs of 1000, 1500, 2000 and 2500 scf/stb. Figure 4.10 shows that the 1.5" tubing can produce the reservoir from a pressure of 1350 psi to 900 psi at a GOR of 1500. Comparing the frictional losses of 2000 and 2500 GORs to that of 1500, it is observed that 2000 and 2500 give higher frictional losses although the same equivalent flow capacities of about 140 bpd and equivalent bottomhole flowing pressure of 950 psi. The 1000 GOR has less frictional loss compared to the other GORs but it can only produce the well from 1350 psi up to a pressure of 1100 psi

where it has to be changed.

Figure 4.11 shows all the GORs with high frictional losses with equivalent flow capacity of about 60 bpd. The frictional effect seems to impede the flow through this tubing. The frictional effect is even worse for the 0.5” tubing with an equivalent flow capacity of about 20 bpd.

Based on the observations, the reservoir is produced with the 1.5” tubing from average reservoir pressure of 1350 psi to 900 psi at a GOR of 1500 scf/stb. At pressure below 900 psi, the frictional loss in the velocity strings may not permit optimal flow capacity and therefore pumping may be the option to consider.

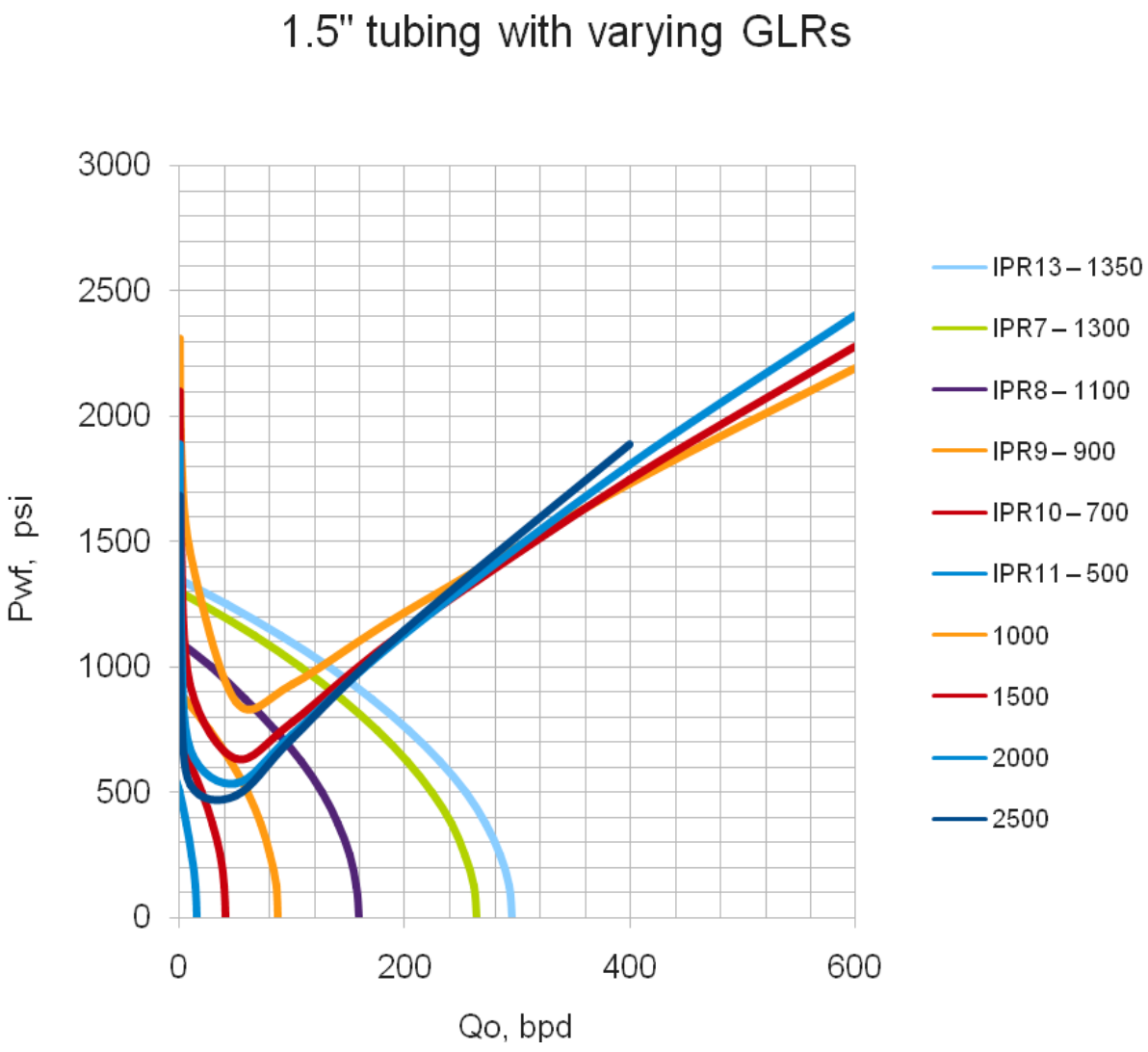

Figure 4.10: Performance of 1.5” tubing under varying GORs

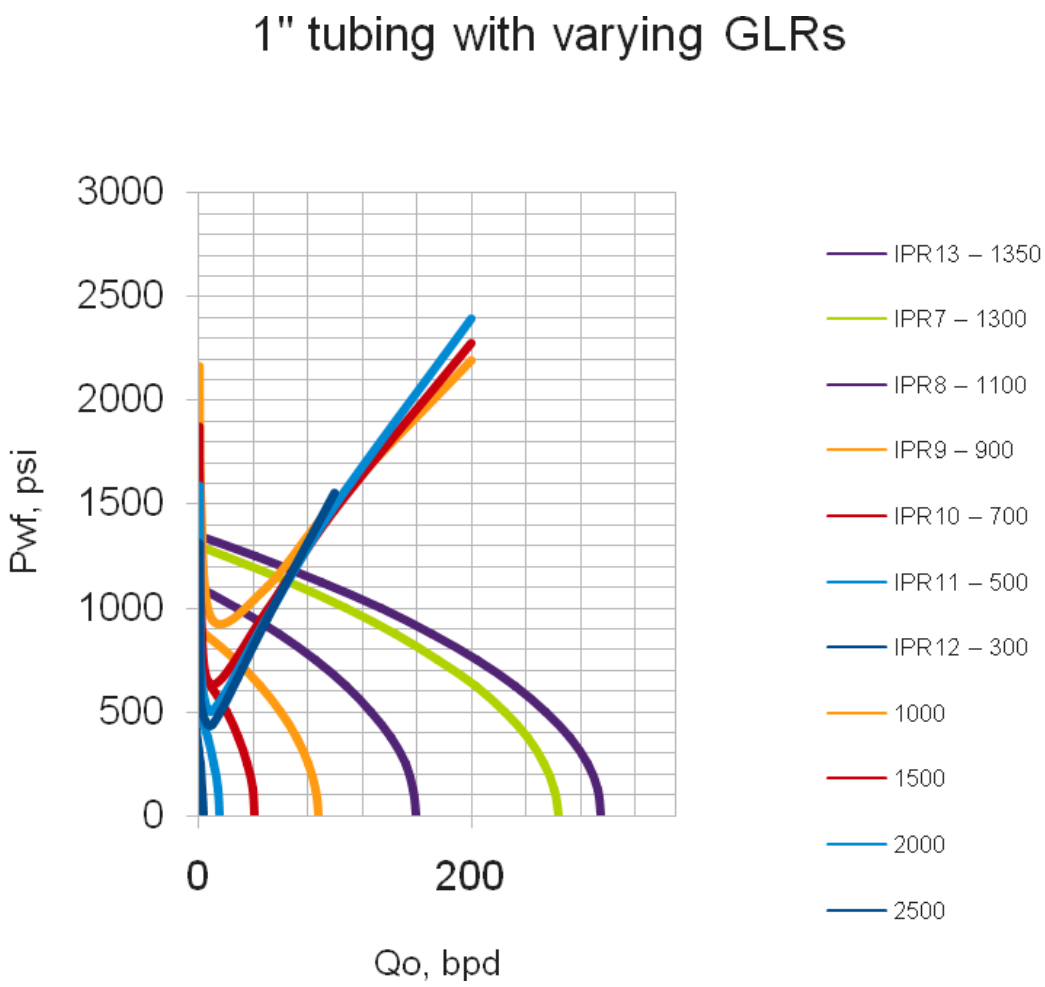

Figure 4.11: Performance of 1" tubing under varying GORs

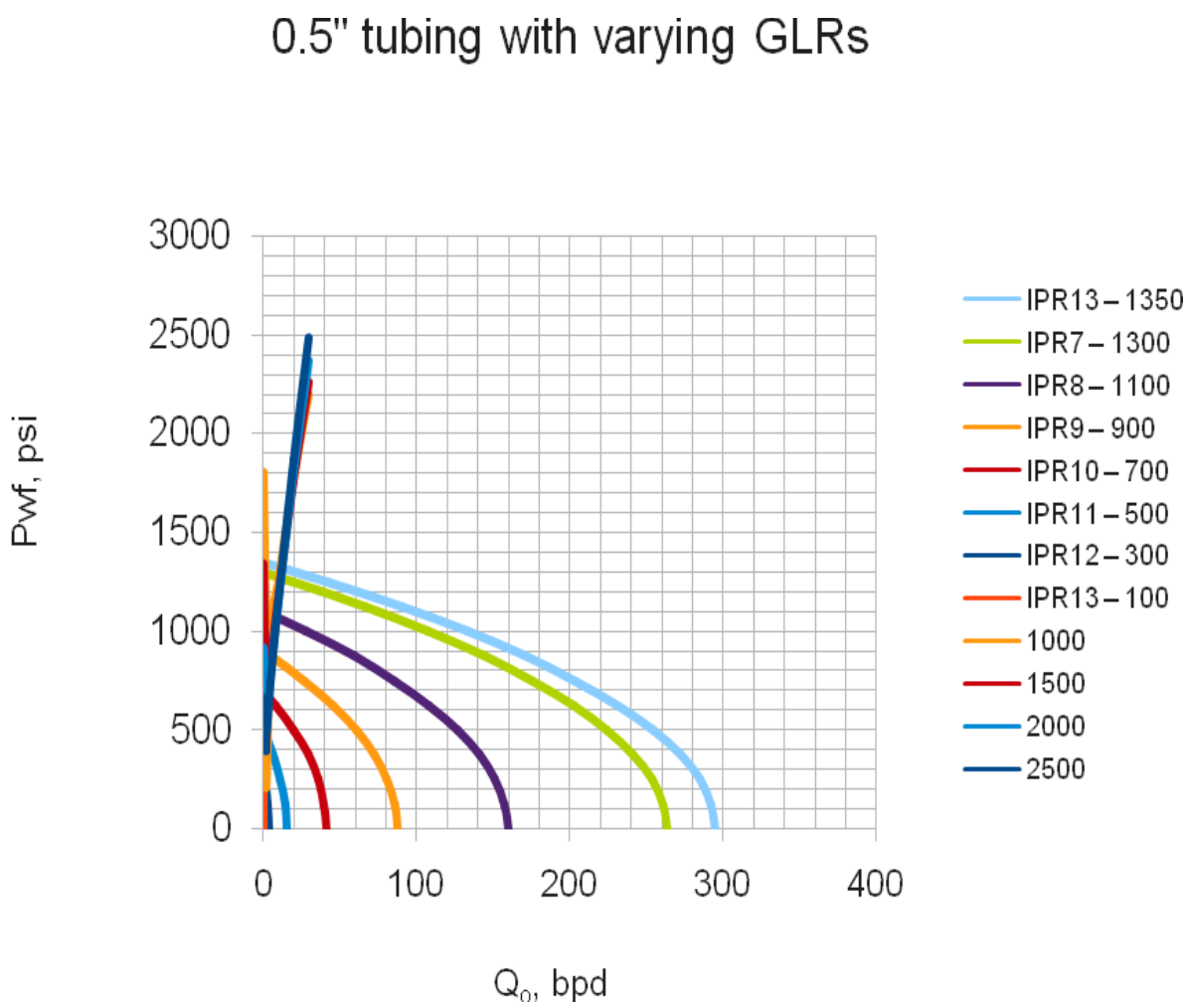

Figure 4.12: Performance of 0.5" tubing under varying GORs

4.8 Relating Performance to Time

Analysis to estimate at what value of average reservoir pressure the producing capacity or deliverability will have declined to is of utmost importance (Beggs, 2003). This type of information needs to be known as a function of time to facilitate development planning or to make economic evaluations (Beggs, 2003). The time to place the well on gas lift and time to install pump or compressors when certain producing capacities can no longer be met is very necessary (Beggs, 2003). The timing of the expenditure of money is required for any economic evaluation of a project or for comparison of projects that require investment (Beggs, 2003).

Figures 4.13 and 4.14 show average reservoir pressure and GOR as functions of cumulative oil produced N_p.

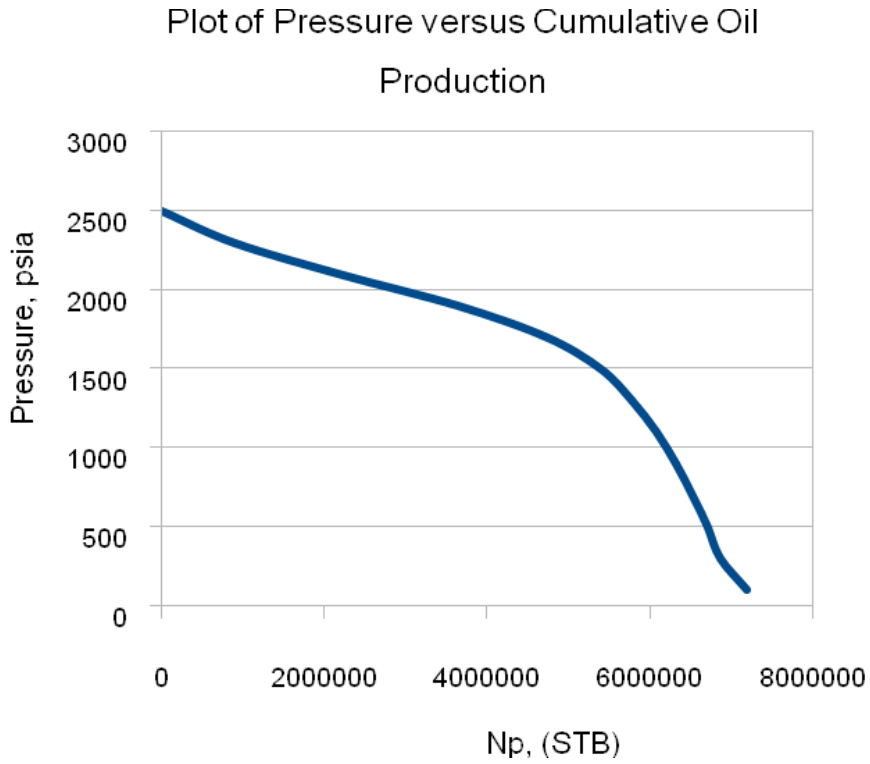

Figure 4.13: Average reservoir pressure as a function of cumulative oil production

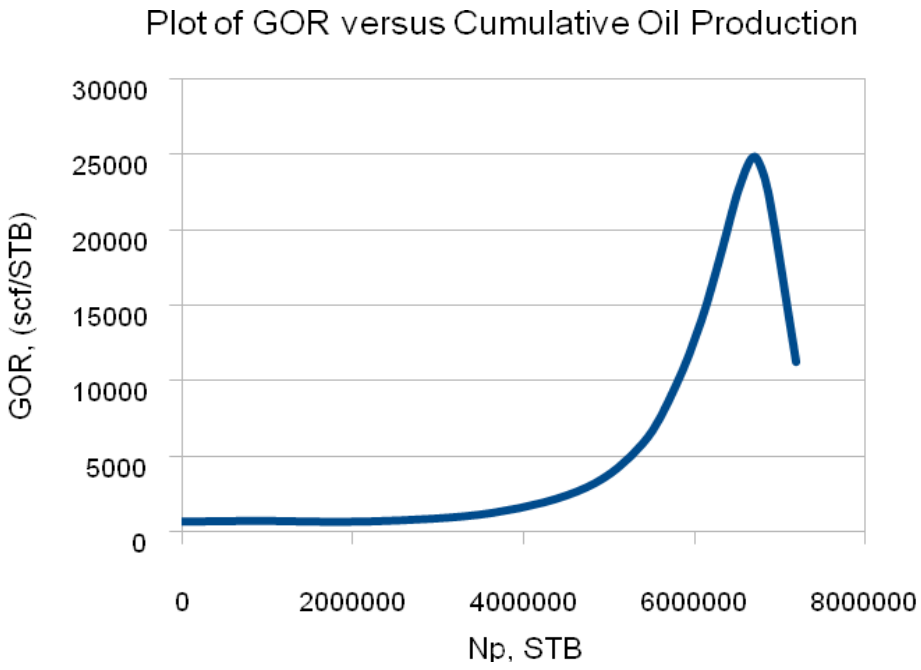

Figure 4.14: GOR development as a function of cumulative oil produced

The table below gives the equivalent flow capacities of the various tubing sizes used and the respective average reservoir pressures.

Table 4.3: Average reservoir pressures and equivalent flow capacities of tubings

Average Reservoir Pressure, P_{avg} (psi)	Equivalent flow Capacitiy, Q_e (bpd)
2500	1350
2300	1050
2100	800
1900	550
1700	490
1500	350
1350	230
1300	140
1100	90
900	50

A plot of equivalent flow capacity as a function of average reservoir pressure is as shown in figure 4.15.

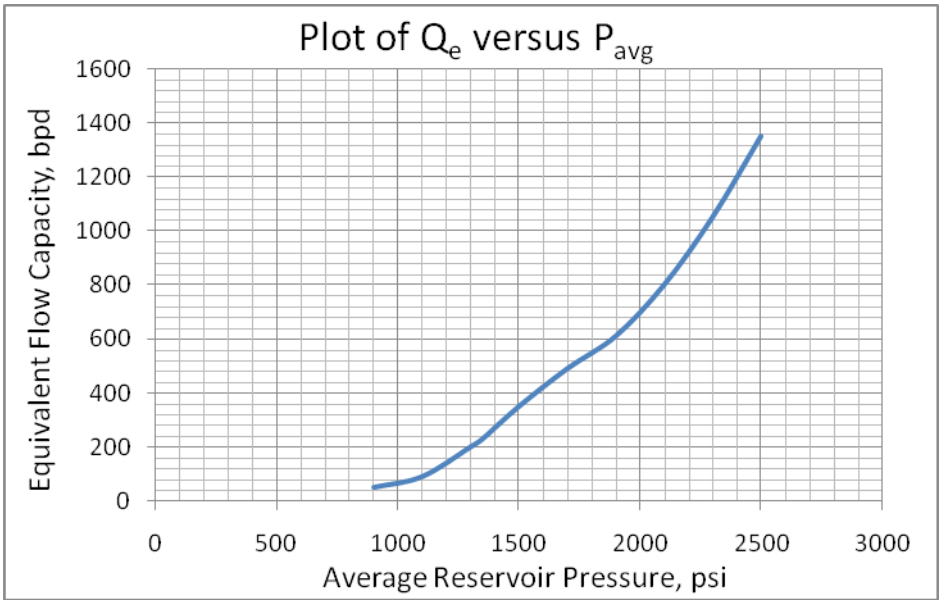

Figure 4.15: Oil producing capacity as a function of reservoir pressure

Table 4.4: Incremental oil production at various reservoir pressures

From table 4.4, selecting an increment of production of 100,000 stb, the average values of reservoir pressure P_{avg} that exist during this producing interval is determined from figure 4.13. Using the value of P_{avg} determined, its corresponding $Qo_{(avg)}$ is determined from figure 4.15. The time increment required to produce the cumulative production increment is calculated as:

$$\Delta t = \frac{\Delta N_p}{Q_{o(avg)}} \tag{4.6}$$

from which the total time is given by:

$$t = \sum \Delta t \tag{4.7}$$

and total cumulative production given by:

$$N_p = \sum \Delta N_p \qquad (4.8)$$

The result of the above discussion is provided in table 4.5 and a plot of performance versus time is shown in figure 4.16 from which the time taken for the oil flowing capacity to reach 50 bpd (that is when pumping will start) is determined to be approximately 17500 days. Figure 4.17 also shows the average pressure decline as a function of time.

Table 4.5 (a): Result of performance as a function of time

$\Delta N_p \times 10^3$ STB	$N_p \times 10^3$ STB	P_{avg} Psi	$Q_{o(avg)}$ bpd	Δt days	t days	Tubing String	GLR Injected scf/stb
100	100	2480	1330	75.19	75.19	2 7/8"	721
100	200	2450	1310	76.34	151.52	2 7/8"	721
100	300	2410	1240	80.65	232.17	2 7/8"	721
100	400	2400	1190	84.03	316.20	2 7/8"	721
100	500	2380	1160	86.21	402.41	2 7/8"	721
100	600	2350	1130	88.50	490.91	2 7/8"	721
100	700	2320	1080	92.59	583.50	2 7/8"	721
100	800	2300	1050	95.24	678.74	2 7/8"	721
100	900	2290	1020	98.04	776.77	2 7/8"	721
100	1000	2260	1000	100.00	876.77	2 7/8"	721
100	1100	2240	970	103.09	979.87	2 7/8"	721
100	1200	2230	960	104.17	1084.03	2 7/8"	721
100	1300	2210	940	106.38	1190.42	2 7/8"	721
100	1400	2200	930	107.53	1297.94	2 7/8"	721
100	1500	2180	900	111.11	1409.06	2 7/8"	721
100	1600	2170	890	112.36	1521.41	2 7/8"	721
100	1700	2160	875	114.29	1635.70	2 7/8"	721
100	1800	2150	860	116.28	1751.98	2 7/8"	721
100	1900	2120	850	117.65	1869.63	2 7/8"	721
100	2000	2105	810	123.46	1993.08	2 7/8"	721
100	2100	2102	805	124.22	2117.31	2 7/8"	721
100	2200	2100	800	125.00	2242.31	2 7/8"	721
100	2300	2090	790	126.58	2368.89	2 7/8"	721
100	2400	2070	760	131.58	2500.47	2 7/8"	721
100	2500	2050	740	135.14	2635.60	2 7/8"	721
100	2600	2035	720	138.89	2774.49	2 7/8"	721
100	2700	2015	690	144.93	2919.42	2 7/8"	721
100	2800	2000	660	151.52	3070.94	2 7/8"	721
100	2900	1990	640	156.25	3227.19	2 7/8"	721
100	3000	1980	620	161.29	3388.48	2 7/8"	721
100	3100	1960	600	166.67	3555.14	2 7/8"	721
100	3200	1950	590	169.49	3724.63	2 7/8"	721
100	3300	1935	580	172.41	3897.05	2 7/8"	721

Table 4.5 (b): Results of performance as a function of time continued

100	3400	1920	575	173.91	4070.96	2 7/8"	721
100	3500	1910	560	178.57	4249.53	2 7/8"	721
100	3600	1900	540	185.19	4434.72	2 7/8"	721
100	3700	1890	530	188.68	4623.40	2 7/8"	721
100	3800	1860	520	192.31	4815.70	2 7/8"	721
100	3900	1840	515	194.17	5009.88	2 7/8"	721
100	4000	1820	510	196.08	5205.96	2 7/8"	721
100	4100	1805	505	198.02	5403.98	2 7/8"	721
100	4200	1800	500	200.00	5603.98	2 7/8"	721
100	4300	1780	490	204.08	5808.06	2 7/8"	721
100	4400	1770	488	204.92	6012.98	2 7/8"	1500
100	4500	1750	485	206.19	6219.16	2 7/8"	1500
100	4600	1720	482	207.47	6426.63	2 7/8"	1500
100	4700	1700	480	208.33	6634.96	2 7/8"	1500
100	4800	1685	470	212.77	6847.73	2 7/8"	1500
100	4900	1670	450	222.22	7069.95	2 7/8"	1500
100	5000	1620	440	227.27	7297.23	2 7/8"	1500
100	5100	1600	430	232.56	7529.78	2 7/8"	1500
100	5200	1550	400	250.00	7779.78	2 7/8"	1500
100	5300	1510	360	277.78	8057.56	2 7/8"	1500
100	5400	1490	340	294.12	8351.68	2 7/8"	1500
100	5500	1420	290	344.83	8696.51	2 7/8"	1500
100	5600	1390	230	434.78	9131.29	1.5"	1500
100	5700	1300	140	714.29	9845.57	1.5"	1500
100	5800	1250	120	833.33	10678.91	1.5"	1500
100	5900	1200	110	909.09	11588.00	1.5"	1500
100	6000	1150	100	1000.00	12588.00	1.5"	1500
100	6100	1100	80	1250.00	13838.00	1.5"	1500
100	6200	1000	60	1666.67	15504.67	1.5"	1500
100	6300	900	50	2000.00	17504.67	1.5"	1500

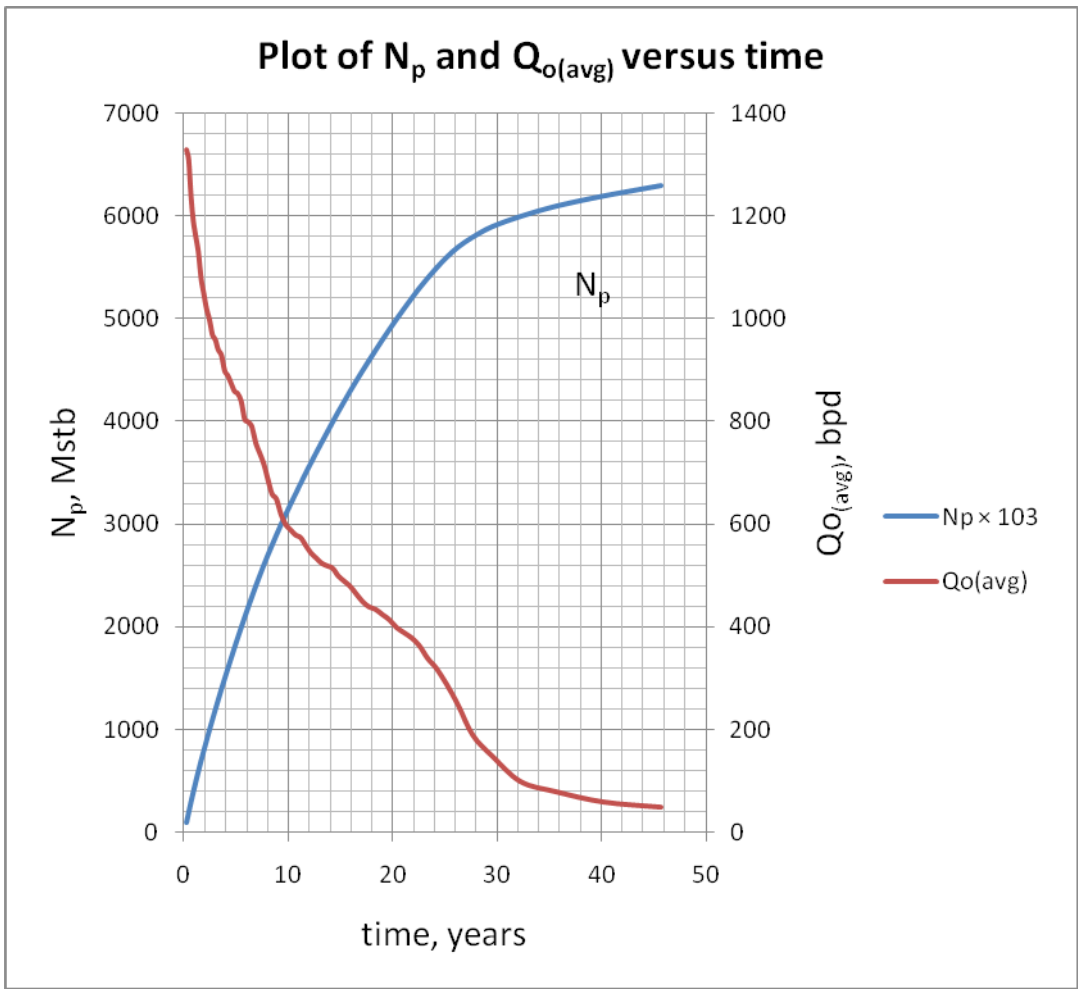

Figure 4.16: Performance versus time

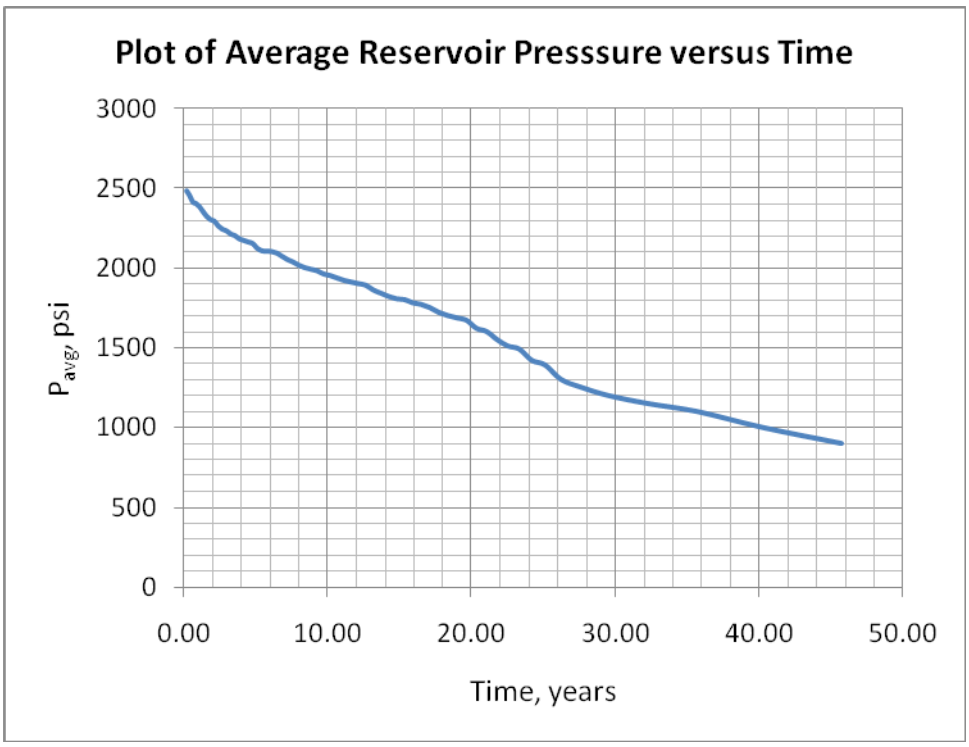

Figure 4.17: Average reservoir pressure as a function of time

A summary of the reservoir production performace with respect to time is given in table 4.6.

Table 4.6: Summary of reservoir production performance as a function time

Chapter 5

5.0 Summary, Conclusions and Recommendations

5.1 Summary

The first objective of this project was to design natural flow and artificial lift tubing strings for the whole life of a well. The focus was placed on solution gas drive reservoirs which are characterised by a rapid and continuous decline of reservoir pressure.

The major disadvantage of this drive mechanism is its low ultimate recovery which suggests that large quantities of oil remain in the reservoir. The primary recovery from such drive was studied and predicted using Muskat's material balance method based on synthetic material balance data. The relationship between cumulative production and average reservoir pressure was determined. It turned out that by depleting the reservoir to 100 psi, a recovery of about of 13% STOIIP could be obtained at a GOR of about 12000 scf/stb. It was also observed that there is enough gas produced to lift the well.

The major disadvantage of this type of drive mechanism makes it a good candidate for secondary recovery applications. Gas lifting was the secondary recovery technique applied in this project to increase the ultimate oil recovery. The energy of expansion of the injected gas propels (pushes) the oil to the surface. The gas also aerates the oil so that the effective density of the fluid is less and, thus, easier to get to the surface.

The size of the tubing string to employ in producing a gas lifted well was also an important aspect of this project. The flowing bottom-hole pressure required to lift the fluids up to the surface is influenced by size of the tubing string and for that matter the time when tubing strings should be replaced as a function of cumulative production was determined. This was achieved by relating performance to time in an attempt to meet the second objective which was to forecast the production of oil as well as the time when tubing strings should be replaced as a function of both

cumulative production and time.

5.2 Conclusions

The following conclusions stem from this dissertation:

- The work in this project confirms the fact that solution – gas drive reservoirs are best candidates for secondary recovery applications due to their low ultimate recovery (about 13% STOIIP).

- For a particular quantity of injected gas for a specific tubing size, no significant oil recovery was obtained. There is always an optimal quantity of gas to be injected for a specific tubing size.

- Velocity strings are associated with high frictional losses which impede oil flow at lower reservoir pressures. As a result, positive displacement pumping was the better option of producing the reservoir at such pressures.

5.3 Recommendations

The following recommendations are suggested.

- Economic evaluation should be included to solve a real life problem. The costs of tubings, pumps, compressors, workover, and injection gas etc. can be evaluated critically to come out with the optimal production pattern of the reservoir.

- Varying tubing head pressure, wellhead pressure and choke sizes can be analyzed to see their effects on the ultimate recovery for a particular production pattern.

- More wells can be included to simulate a more practical situation and the performance with time analyzed.

Appendix A – Beggs and Brill Program

The Beggs and Brill program (Prado, 2008) is a spreadsheet program developed to obtain the IPR and OPR curves. The Beggs and Brill correlation enables the calculation of the pressure gradient as a function of other production variables like pipe diameter, GLR and gas and oil flow rates. The terms and their equations that go into the Beggs and Brill program are as follows:

The gas solubility in oil (R_{so})

This is calculated using Standing Correlation as outlined in equation A.1.

$$R_{SO} = \gamma_g \left[\left(\frac{P+14.7}{18.2} + 1.4\right) 10^{0.0125 \cdot API - 0.00091T}\right]^{1.2048} \quad \text{(A.1)}$$

where R_{so} is in scf/day,

P is in psig,

T is in ˚F

The gas solubility in water (R_{sw})

This is calculated using Culberson and Maketta Correlation as outlined below in equation A.2.

$$R_{SO} = A + B(P + 14.7) + C(P + 14.7)^2 \quad \text{(A.2)}$$

where A, B, and C are given by equations A.3, A.4, and A.5 respectively.

$$A = 8.15839 - 6.12265 \times 10^{-2}T + 1.91663 \times 10^{-4}T^2 - 2.1654 \times 10^{-7}T^3 \quad \text{(A.3)}$$

$$B = 1.01021 \times 10^{-2} - 7.44241 \times 10^{-5}T + 3.05553 \times 10^{-7}T^2 - 2.94883 \times 10^{-10}T^3 \quad \text{(A.4)}$$

$$C = [-9.025 + 0.1302T - 8.534 \times 10^{-4}T^2 + 2.341 \times 10^{-6}T^3 - 2.37 \times 10^{-9}T^4] \times 10^{-7} \quad \text{(A.5)}$$

Water cut (WC)

The water cut if not known is determined using equation A.6 below.

$$WC = \left(\frac{q_w}{q_o + q_w}\right) \quad \text{(A.6)}$$

where q_w is water flowrate and q_o is the oil flowrate all in stbpd.

Production GOR and production GLR

Producing gas – oil ratio (GOR_p) is determined from equation A.7 knowing the producing gas – liquid ratio (GLR_p).

$$GLR_p = GOR_p(1 - WC) \quad \text{(A.7)}$$

and

$$GLR_p - (1 - WC)R_{SO}(P_b) - WCR_{SW}(P_b) = 0 \quad \text{(A.8)}$$

The mixture bubble point is the solution to the equation A.8.

Free gas-liquid ratio (GLR_{free} – Gas Mass Balance)

From gas mass balance, the free gas-liquid-ratio (GLR_{free}) is given in two conditions as:

(A.9)

where GLR_{free}, GLR_p, R_{so}, *and* R_{sw} are all in scf/stb and WC is a fraction.

Appendix B – Inflow Performance Relationship (IPR) from Production Tests

Production test data are used to determine the numerical values of the IPR parameters**.** There are 4 cases depending on the location of the production test bottom hole flowing pressure with respect to the bubble point pressure. These are:

- Both tests above the bubble point
- One test above and one test below the bubble point
- Two tests below the bubble point for a under - saturated reservoir
- Two tests below the bubble point for a saturated reservoir

CASE 1: Both tests above the bubble point pressure as illustrated by figure B.1

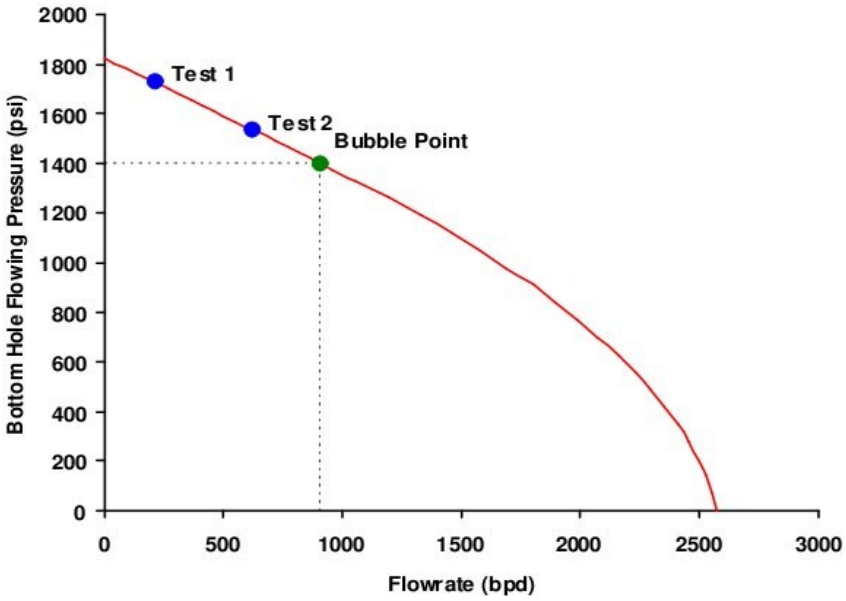

Figure B.1: Both production tests above the bubble point

In this case, the linear IPR equation is used for both tests and solved for the average reservoir pressure and productivity index. After this is done, the continuity and smoothness equations can be used to calculate the bubble point flowrate and the absolute open flow.

The necessary parameters are obtained as follows:

$$\overline{P} = \frac{q_2 P_1 - q_1 P_2}{q_2 - q_1} \quad \text{(B.1)}$$

$$J ¿ = \frac{q_2 - q_1}{P_1 - P_2} \quad \text{(B.2)}$$

$$\frac{q - q_b}{q_{\max} - q_b} = 1 + b\left(\frac{P_{wf}}{\overline{P}'}\right) - (1+b)\left(\frac{P_{wf}}{\overline{P}'}\right)^2 \text{ (non – linear portion)} \quad \text{(B.3)}$$

$$q_b = J ¿ (\overline{P} - P_b) \quad \text{(B.4)}$$

$$q_b = J ¿ (\overline{P} - P_{wf}) \quad \text{(linear portion)} \quad \text{(B.5)}$$

$$q_{\max} = \frac{J ¿ \overline{P}'}{2+b} + q_b \quad \text{(B.6)}$$

$$\overline{P}' = P_b \quad \text{(B.7)}$$

CASE 2: Tests in opposite sides of the bubble point as illustrated by figure B.2

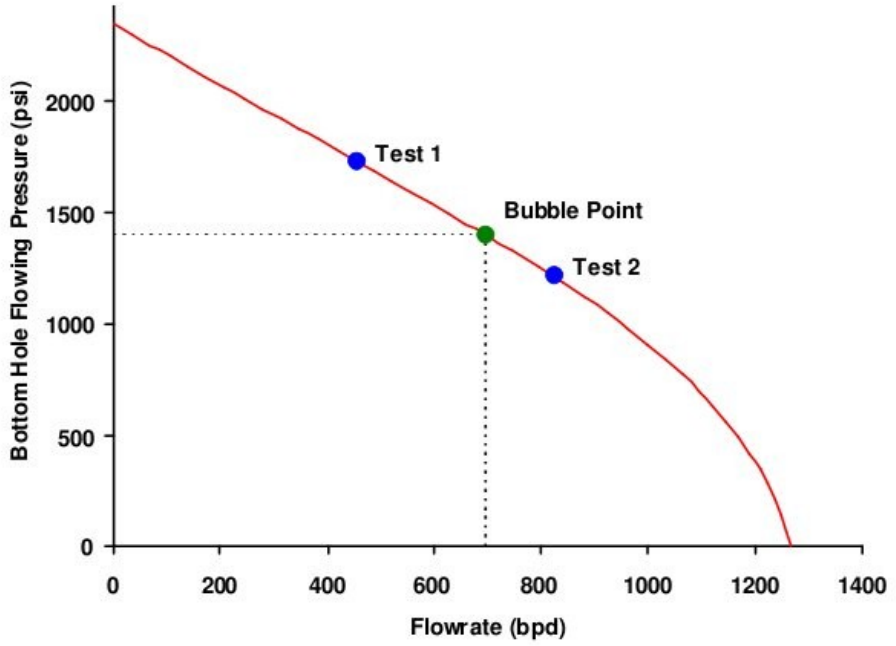

Figure B.2: Tests in opposite sides of the bubble point

In this case, the linear and the parabolic IPR equations are used for the corresponding tests and solved for the four parameters simultaneously.

The necessary parameters are obtained as follows:

$$J^{¿}=\frac{(2+b)(q_2-q_1)}{(2+b)P_1+bP_2-(1+b)\left(P_b+\frac{P_{2^2}}{P_b}\right)} \qquad \text{(B.8)}$$

$$\overline{P}=\frac{q_1}{J^{¿}}+P_1 \qquad \text{(B.9)}$$

$$\overline{P}'=P_b \qquad \text{(B.10)}$$

$$q_b=J^{¿}(\overline{P}-P_b) \qquad \text{(B.11)}$$

$$q_{\max}=\frac{J^{¿}\overline{P}'}{2+b}+q_b \qquad \text{(B.12)}$$

$$q_b=J\,¿(\overline{P}-P_{wf}) \quad \text{(linear portion)} \qquad \text{(B.13)}$$

$$\frac{q-q_b}{q_{\max}-q_b}=1+b\left(\frac{P_{wf}}{\overline{P}'}\right)-(1+b)\left(\frac{P_{wf}}{\overline{P}'}\right)^2 \quad \text{(non – linear portion)} \qquad \text{(B.14)}$$

CASES 3 and 4: In those cases both tests are below the bubble point pressure as illustrated by figures B.3 and B.4.

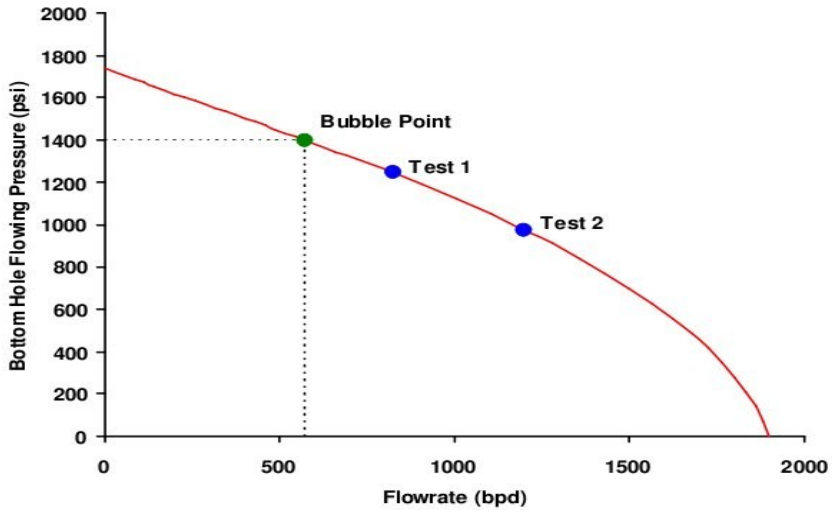

Figure B.3: Both tests below the bubble point pressure

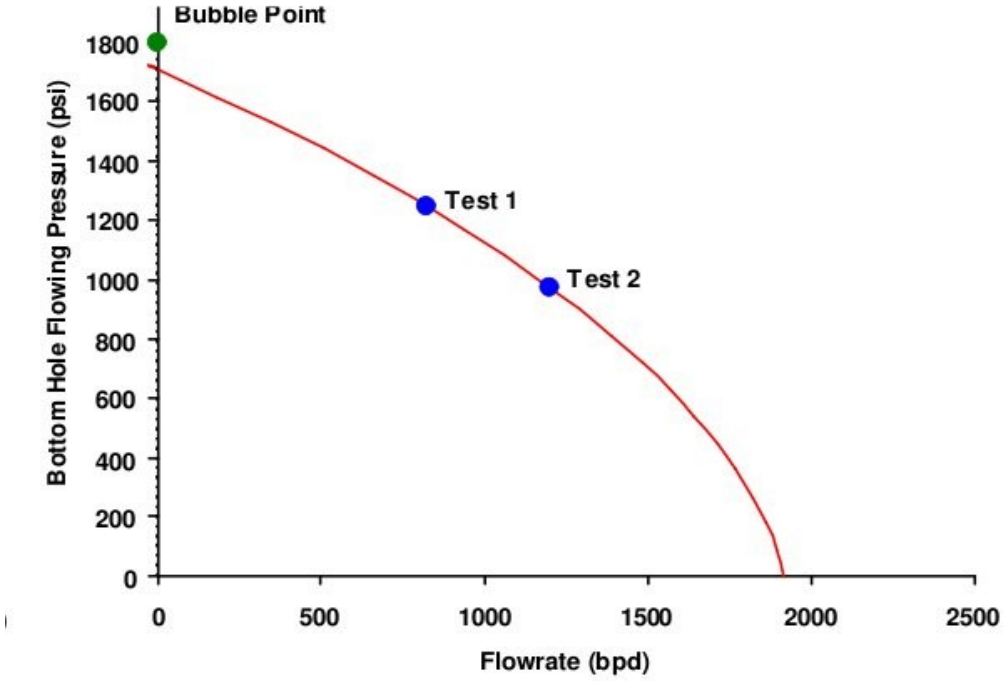

Figure B.4: Both tests below the bubble point pressure

It cannot be told in advance which case it is when only the production tests data and bubble point pressure are known. Therefore, a hypothesis is tested and its validity verified. First assume that we have Case 3. If this is correct, the bubble point flowrate should be greater than zero. If the calculated bubble point flowrate is less than zero we have Case 4 and the results should be recalculated.

The necessary parameters for case 3 are obtained as follows:

$$q_b = \frac{\left(1+b\frac{P_2}{P_b}-(1+b)\left(\frac{P_2}{P_b}\right)^2\right)q_1-\left(1+b\frac{P_1}{P_b}-(1+b)\left(\frac{P_1}{P_b}\right)^2\right)q_2}{\left(1+b\frac{P_2}{P_b}-(1+b)\left(\frac{P_2}{P_b}\right)^2\right)-\left(1+b\frac{P_1}{P_b}-(1+b)\left(\frac{P_1}{P_b}\right)^2\right)} \geq 0 \qquad \text{(B.15)}$$

$$J^{i} = \frac{(2+b)(q_2-q_b)}{P_b\left(1+b\frac{P_2}{P_b}-(1+b)\left(\frac{P_2}{P_b}\right)^2\right)} \qquad \text{(B.16)}$$

$$\overline{P} = P_b + \frac{q_b}{J^{i}} \qquad \text{(B.17)}$$

$$\overline{P}' = P_b \qquad \text{(B.18)}$$

$$q_{\max}=\frac{J^{¿}\overline{P}'}{2+b}+q_b \tag{B.19}$$

$$q_b=J\,¿(\overline{P}-P_{wf}) \quad \text{(linear portion)} \tag{B.20}$$

$$\frac{q-q_b}{q_{\max}-q_b}=1+b\left(\frac{P_{wf}}{\overline{P}'}\right)-(1+b)\left(\frac{P_{wf}}{\overline{P}'}\right)^2 \quad \text{(non–linear portion)} \tag{B.21}$$

The necessary parameters for case 4 are obtained as follows:

$$\frac{\left(1+b\frac{P_2}{P_b}-(1+b)\left(\frac{P_2}{P_b}\right)^2\right)q_1-\left(1+b\frac{P_1}{P_b}-(1+b)\left(\frac{P_1}{P_b}\right)^2\right)q_2}{\left(1+b\frac{P_2}{P_b}-(1+b)\left(\frac{P_2}{P_b}\right)^2\right)-\left(1+b\frac{P_1}{P_b}-(1+b)\left(\frac{P_1}{P_b}\right)^2\right)}\le 0 \tag{B.22}$$

$$\overline{P}=\frac{-b(q_1P_2-q_2P_1)-\sqrt{b^2(q_1P_2-q_2P_1)^2+4(1+b)(q_1-q_2)(q_1P_{2^2}-P_{1^2})}}{2(q_1-q_2)} \tag{B.23}$$

$$q_{\max}=\frac{q_1}{1+b\left(\frac{P_1}{\overline{P}}\right)-(1+b)\left(\frac{P_1}{\overline{P}}\right)^2}=\frac{q_2}{1+b\left(\frac{P_2}{\overline{P}}\right)-(1+b)\left(\frac{P_2}{\overline{P}}\right)^2} \tag{B.24}$$

$$q_b=0 \tag{B.25}$$

$$\overline{P}'=\overline{P} \tag{B.26}$$

$$J^{¿}=(2+b)\frac{q_{\max}-q_b}{\overline{P}'} \tag{B.27}$$

$$\frac{q-q_b}{q_{\max}-q_b}=1+b\left(\frac{P_{wf}}{\overline{P}'}\right)-(1+b)\left(\frac{P_{wf}}{\overline{P}'}\right)^2 \quad \text{(non–linear portion)} \tag{B.28}$$

Bibliography

Beggs, D., *Production Optimization Using Nodal Analysis, S*econd Edition, OGCI and Petroskills Publications, Tulsa, Oklahoma, pp. 150 - 153, 2003.

Boyun, G., Lyons, W. C., and Ghalambor, A., *Petroleum Production Engineering,* Elsevier Science and Technology Books, 287 pp., 2007.

Craft, B. C., and Hawkins, M., *Applied Petroleum Reservoir Engineering, S*econd Edition, Prentice – Hall, Inc., New Jersey, pp. 370 – 375, 1991.

Cosentino, L., Integrated *Reservoir Studies,* Technip Editions, Paris, pp. 182 – 187, 2001.

Dake, L. P., *Fundamentals of Reservoir Engineering*, Elsevier, Amsterdam, The Netherlands, 1978.

Dake, L. P., *The Practice* o*f Reservoir Engineering*, Revised Edition, Elsevier, pp. 86 – 109, 1994.

Golan, M., and Whitson, C. H., *Well Performance,* Second Edition, Prentice – Hall, Inc., 1995.

Lyons, W. C., *Standard Handbook of Petroleum & Natural Gas Engineering,* Vol. 1, Gulf Publishing Company, Houston, Texas, 1996.

Lea, J. F., Nickens, H. V., and Mike, R., *Gas Well Deliquification*, Second Edition, Gulf Professional Publishing, 30 Corporate Drive, Suite 400, Burlington, MA 01803, USA, 588 pp., 2008.

Mohamed, E., Ahmed, E. H., Fattah, K. A., and El-Sayed, A. M. E., "New Inflow Performance Relationship for Solution-Gas Drive Oil Reservoirs," paper SPE 124041 presented at the 2009 SPE Annual Technical Conference and Exhibition held in New Orleans, Louisiana, USA, 4–7 October 2009.

Oudeman, P., "On the Flow Performance of Velocity Strings To Unload Wet Gas Wells," paper SPE 104605 presented at the 15th SPE Middle East Oil & Gas Show and Conference held in Bahrain International Exhibition Centre, Kingdom of Bahrain, 11 – 14 March, 2007.

Prado, M., "Two Phase Flow and Nodal Analysis," Lecture material delivered at the

African University of Science and Technology, 2008.

Tarek, A., *Reservoir Engineering Handbook,* Second Edition, Gulf Professional Publishing, 2001.